

Award Number: W81XWH-10-1-0249

TITLE: Novel Therapeutic Approaches Toward Treating Prostate Cancer

PRINCIPAL INVESTIGATOR: Andrew S. Kraft, MD

CONTRACTING ORGANIZATION: Medical University of South Carolina
Charleston, SC 29425

REPORT DATE: May 2012

TYPE OF REPORT: Annual

PREPARED FOR: U.S. Army Medical Research and Materiel Command
Fort Detrick, Maryland 21702-5012

DISTRIBUTION STATEMENT: Approved for Public Release;
Distribution Unlimited

The views, opinions and/or findings contained in this report are those of the author(s) and should not be construed as an official Department of the Army position, policy or decision unless so designated by other documentation.

REPORT DOCUMENTATION PAGE

Form Approved
OMB No. 0704-0188

Public reporting burden for this collection of information is estimated to average 1 hour per response, including the time for reviewing instructions, searching existing data sources, gathering and maintaining the data needed, and completing and reviewing this collection of information. Send comments regarding this burden estimate or any other aspect of this collection of information, including suggestions for reducing this burden to Department of Defense, Washington Headquarters Services, Directorate for Information Operations and Reports (0704-0188), 1215 Jefferson Davis Highway, Suite 1204, Arlington, VA 22202-4302. Respondents should be aware that notwithstanding any other provision of law, no person shall be subject to any penalty for failing to comply with a collection of information if it does not display a currently valid OMB control number. **PLEASE DO NOT RETURN YOUR FORM TO THE ABOVE ADDRESS.**

1. REPORT DATE May 2012		2. REPORT TYPE Annual		3. DATES COVERED 15 Apr 2011 - 14 Apr 2012	
4. TITLE AND SUBTITLE Novel Therapeutic Approaches Toward Treating Prostate Cancer				5a. CONTRACT NUMBER	
				5b. GRANT NUMBER W81XWH-10-1-0249	
				5c. PROGRAM ELEMENT NUMBER	
6. AUTHOR(S) Andrew S. Kraft, MD E-Mail: kraft@musc.edu				5d. PROJECT NUMBER	
				5e. TASK NUMBER	
				5f. WORK UNIT NUMBER	
7. PERFORMING ORGANIZATION NAME(S) AND ADDRESS(ES) Medical University of South Carolina Charleston, SC 29425				8. PERFORMING ORGANIZATION REPORT NUMBER	
9. SPONSORING / MONITORING AGENCY NAME(S) AND ADDRESS(ES) U.S. Army Medical Research and Materiel Command Fort Detrick, Maryland 21702-5012				10. SPONSOR/MONITOR'S ACRONYM(S)	
				11. SPONSOR/MONITOR'S REPORT NUMBER(S)	
12. DISTRIBUTION / AVAILABILITY STATEMENT Approved for public release; distribution unlimited					
13. SUPPLEMENTARY NOTES					
14. ABSTRACT: The Pim protein kinase is over expressed in prostate cancer. To clarify the role of this protein in regulating normal prostate and cancer growth we have investigated its mechanism of action. We demonstrate that inhibition of AKT in prostate cancer cell lines induces the expression of multiple receptor tyrosine kinases (RTKs), but increases the protein levels of serine threonine protein kinase Pim-1. Pim-1 activity is identified as essential in the feedback regulation of RTK levels by AKT inhibition. Pim-1 appears to control RTKs by regulating the translation of these proteins in a cap-independent mechanism. Both tissue culture and animal experiments demonstrate that the combination of AKT and Pim inhibitors provide synergistic inhibition of tumor growth. Thus, this combination therapy has the potential activity to be developed as a prostate cancer treatment.					
15. SUBJECT TERMS Pim Kinases, Prostate Cancer, AKT inhibition, Mouse, Prostate Stem Cells					
16. SECURITY CLASSIFICATION OF: U			17. LIMITATION OF ABSTRACT UU	18. NUMBER OF PAGES 34	19a. NAME OF RESPONSIBLE PERSON USAMRMC
a. REPORT U	b. ABSTRACT U	c. THIS PAGE U			19b. TELEPHONE NUMBER (include area code)

Table of Contents

	<u>Page</u>
Introduction.....	4
Body.....	4
Key Research Accomplishments.....	6
Reportable Outcomes.....	7
Conclusion.....	8
Appendix.....	9
Supporting Data.....	26

INTRODUCTION (Subject, purpose, and scope)

The overexpression of the serine/threonine Pim protein kinase in normal or cancerous prostate cells stimulates the growth of these cells. Pim is over expressed in human prostate cancer, and its level may parallel the onset of metastatic disease. In animal models the expression of the c-Myc protein is associated with increased Pim protein levels. Overexpression of Pim-1 in murine prostate stem cells increases their growth. Thus, data from tissue culture, human and animal prostate cancer implicates the Pim protein in prostate tumorigenesis. In this application we suggested that Pim regulates the levels of the cell cycle inhibitor p27. The ability of Pim to drive down the level of p27 suggests that this could be important in affecting tumor growth. We have hypothesized that this decrease will coordinate with elevated c-Myc in tumor cells to drive tumor growth. Our laboratory has developed novel benzylidene thiazolidine-2,4 diones, (D5, SMI-4a) that inhibit the activity of Pim kinase. These agents reverse Pim activity and allow the level of p27 to rise. This protein will then function to inhibit tumor growth. The first subtask of this grant was to understand the mechanism by which Pim protein kinases regulate p27. We have completed this work and published the mechanism in the Journal of Biological Chemistry (see reportable outcomes) in which we detail the ability of Pim to phosphorylate both Skp-2 and Cdc27. Finally, the second subtask of this proposal was to evaluate the anti-tumor activity of the Pim protein kinases and decipher whether inhibition of one or more isoforms was necessary to inhibit tumor growth.

BODY

Our efforts have focused on specific items in the Statement of Work to allow us to bring together data that will explain how Pim inhibitors may be used to treat prostate cancer. Two significant publications have arisen from this work and are having making impressive impact on the development of Pim inhibitors. For the current work we have focused on subtask 2b that was to be accomplished in the current year two of this application. Rather than reviewing the progress of the previous tasks we will focus on the new information generated in this progress period.

Task 2b to be completed in year 2

An important approach to treating prostate cancer is targeting prostate cancer treatment is to block the AKT signaling pathway. Through mutation of PTEN, PI3 kinase, or AKT itself, this pathway is activated in prostate cancer in 50-70% of patients. For this reason pharmaceutical companies have invested in developing molecules that inhibit these enzymes. Importantly, we find that when AKT inhibitors are used to treat prostate cancer that they cause a feedback stimulation of the levels of cell surface receptor tyrosine kinases (RTKs). This increase in RTKs will then enhance AKT stimulation, blunting the effect of these drugs (Fig. 1) and creating a resistance mechanism. We find that the AKT inhibitor, GSK690693, not only increases RTK levels but of importance also elevates the levels of Pim-1, but not Pim-2, or Pim-3 (Fig. 1). Results demonstrate that the AKT inhibitor (GSK-690693) increases Pim-1 transcriptionally (Fig. 2). The mechanisms by which AKT inhibitors raise the levels of Pim-1 appear to not involve the Foxo transcription factors. Pim-1 is degraded by the ubiquitin pathway, and this could play a role in the regulation of the levels of this protein. Since the Pim-1 mRNA contains a suggestive mRNA IRES sequence, we cannot rule out the possibility that Pim-1 levels are controlled by other mechanisms.

Importantly, we have discovered that inhibiting or decreasing the level of Pim-1, blocks the feedback ability of AKT inhibitors to elevate the levels of RTKs (Fig. 3). This can be shown using genetic knockouts (Fig. 3c), siRNAs (Fig. 3a) or the small molecule Pim-1 inhibitor described above (Fig. 3b), SMI-4a. This may suggest that inhibiting only Pim-1 will be sufficient to block the feedback increase in RTKs caused by AKT inhibitors. We also find that in the absence of AKT inhibitors decreasing the level of Pim-1 causes a fall in the level of RTKs. This result suggests that Pim-1 plays an important role in the control of protein levels and may suggest a broader control of mRNA transcription and/or protein translation.

The mechanism by which Pim-1 regulates RTKs is unknown. Inhibitors of the mTORC1 activity do not block this increase suggesting that it is cap-independent. We find that both GSK690693 and Pim-1 are able to stimulate translation from an internal ribosome entry site (IRES). By cloning the 5' upstream region of c-Met we demonstrate that it contains an IRES. This experiment involved cloning the IRES sequence of c-Met in front of firefly luciferase and then examining whether Pim-1 could regulate this sequence (Fig. 4, 5). In this vector the SV-40 promoter controlled the translation of the renilla luciferase. Decreases in Pim-1 levels decreased firefly luciferase while increasing Pim-1 increases this readout. Based on these results we have combined small molecule Pim-1 and AKT inhibitors and shown that they can synergistically inhibit cell growth on plastic, soft-agar growth of prostate cancer cells, and block the subcutaneous growth of tumors in nude mice (Fig. 6). These data suggest that this combination therapy possibly by blocking feedback regulation of RTKs can inhibit tumor growth. These compounds could form a novel drug therapy for prostate cancer.

KEY RESEARCH ACCOMPLISHMENTS

- 1- Inhibition of AKT in prostate cancer cells elevates the levels of both Pim-1, but not Pim-2 or Pim-3, and cell surface receptor tyrosine kinases (RTKs).
- 2- Inhibition of Pim-1 with inhibitor, SMI-4a, or decreasing the level of Pim-1 protein inhibited the ability of AKT inhibitors to induce RTKs.
- 3- AKT inhibition leads to the transcriptional up regulation of Pim-1.
- 4- Pim-1 or small molecule AKT inhibitors are able to increase the levels of RTKs by a cap-independent mechanism.
- 5- The combination of a Pim-1 and AKT inhibitor is synergistic in killing prostate cancer cells in tissue culture and in an animal model.

REPORTABLE OUTCOMES

Abstracts

Bo Cen, Sandeep Mahajan, and Andrew S. Kraft Overcoming Resistance to Inhibitors of the AKT Protein Kinases by Targeting the Pim Protein Kinase Pathway. *Advances in Prostate Cancer Research* February 6-9, 2012 Abstract C12, Page 133

Papers

Cen B, Sandeep M, Zemskova M, Beharry Z, Lin YW, Cramer SD, Lilly M, and **Kraft AS**. Regulation of SKP2 Levels by the PIM-1 Protein Kinase. *J Biol Chem* 285 (38): 29128-29137, 2010. PMID 20663873, PMCID: PMC2937943

Beharry Z, Mahajan S, Zemskova M, Lin Y-W, Tholanikunnel B, Xia Z, Smith CD, and **Kraft AS**. The Pim protein kinases regulate energy metabolism and cell growth. *Proceedings of the National Academy of Sciences*. 108:528-533, 2011, PMID: 21187426, PMCID: PMC3021022

CONCLUSIONS

The serine threonine Pim protein kinases are overexpressed in prostate cancers and promote cell growth and survival. The PI3K/AKT pathway is activated in over 60% of human prostate cancers, suggesting that compounds that inhibit this pathway may be useful for therapy. However, accumulating evidence indicates that feedback regulation in response to inhibition of PI3K/AKT signaling pathway may attenuate antitumor activity of inhibitors by increasing the level of cell surface receptor tyrosine kinases (RTKs). We demonstrate that inhibition of AKT in prostate cancer cell lines not only induces the expression of multiple RTKs, but increases the protein levels of serine threonine protein kinase Pim-1. Pim-1 activity is identified as essential in the feedback regulation of RTK levels by AKT inhibition. Knockdown of Pim-1 expression or inhibition of Pim-1 activity with small molecules abrogates the induction of RTKs and overexpression of Pim-1 increases RTK levels. Experiments using dual luciferase vectors demonstrate that Pim-1 controls expression of c-Met and other RTKs at the translational level by modulating IRES activity in a cap-independent manner. Both tissue culture and animal experiments demonstrate that the combination of AKT and Pim inhibitors provides synergistic inhibition of tumor growth. Our results demonstrate that Pim-1 is a novel mediator of resistance to AKT inhibition, and that targeting Pim kinases significantly improves the efficacy of AKT inhibitors in anticancer therapy. This combination therapy could be brought into the clinic and suggests that inhibition of Pim-1 and not Pim-2 or 3 might be sufficient as dual therapy.

APPENDIX

1. Cen B, Sandeep M, Zemskova M, Beharry Z, Lin YW, Cramer SD, Lilly M, and **Kraft AS**. Regulation of SKP2 Levels by the PIM-1 Protein Kinase. *J Biol Chem* 285 (38): 29128-29137, 2010. PMID 20663873, PMCID: PMC2937943
2. Beharry Z, Mahajan S, Zemskova M, Lin Y-W, Tholanikunnel B, Xia Z, Smith CD, and **Kraft AS**. The Pim protein kinases regulate energy metabolism and cell growth. *Proceedings of the National Academy of Sciences*. 108:528-533, 2011. PMID: 21187426, PMCID: PMC3021022

Regulation of Skp2 Levels by the Pim-1 Protein Kinase^{*S}

Received for publication, April 22, 2010, and in revised form, July 22, 2010. Published, JBC Papers in Press, July 27, 2010, DOI 10.1074/jbc.M110.137240

Bo Cen[‡], Sandeep Mahajan[§], Marina Zemskova[¶], Zanna Beharry^{||}, Ying-Wei Lin^{**}, Scott D. Cramer^{††}, Michael B. Lilly^{§§}, and Andrew S. Kraft^{†§1}

From the [‡]Department of Medicine, [§]Hollings Cancer Center, and the Departments of [¶]Cell and Molecular Pharmacology, ^{||}Pharmaceutical and Biomedical Sciences, and ^{**}Pediatrics, Medical University of South Carolina, Charleston, South Carolina 29425, the ^{††}Department of Cancer Biology and Comprehensive Cancer Center, Wake Forest University School of Medicine, Winston-Salem, North Carolina 27157, and the ^{§§}Division of Hematology/Oncology, Department of Medicine, University of California, Irvine, California 92868

The Pim-1 protein kinase plays an important role in regulating both cell growth and survival and enhancing transformation by multiple oncogenes. The ability of Pim-1 to regulate cell growth is mediated, in part, by the capacity of this protein kinase to control the levels of the p27, a protein that is a critical regulator of cyclin-dependent kinases that mediate cell cycle progression. To understand how Pim-1 is capable of regulating p27 protein levels, we focused our attention on the SCF^{Skp2} ubiquitin ligase complex that controls the rate of degradation of this protein. We found that expression of Pim-1 increases the level of Skp2 through direct binding and phosphorylation of multiple sites on this protein. Along with known Skp2 phosphorylation sites including Ser⁶⁴ and Ser⁷², we have identified Thr⁴¹⁷ as a unique Pim-1 phosphorylation target. Phosphorylation of Thr⁴¹⁷ controls the stability of Skp2 and its ability to degrade p27. Additionally, we found that Pim-1 regulates the anaphase-promoting complex or cyclosome (APC/C complex) that mediates the ubiquitination of Skp2. Pim-1 phosphorylates Cdh1 and impairs binding of this protein to another APC/C complex member, CDC27. These modifications inhibit Skp2 from degradation. Marked increases in Skp2 caused by these mechanisms lower cellular p27 levels. Consistent with these observations, we show that Pim-1 is able to cooperate with Skp2 to signal S phase entry. Our data reveal a novel Pim-1 kinase-dependent signaling pathway that plays a crucial role in cell cycle regulation.

The Pim family of serine/threonine kinases regulates the growth and survival of cells and plays a role in enhancing the transformed phenotype driven by oncogenes, including Myc and Akt (1–3). As the Pim kinases are elevated in human tumors, including prostate, leukemia, and pancreatic cancer, and appear to be useful in distinguishing benign from malignant tumors (4), it has been suggested that they play a role in the growth or progression of these malignancies (5, 6). In prostate cancer, decreased Pim-1 expression correlated significantly with measures of poor outcome and was found to be associated with a higher cumulative rate of prostate-specific antigen fail-

ure and a strong predictor of prostate-specific antigen recurrence (4). Based on crystal structural analysis (7–11), the Pim family of kinases appears to be constitutively active and not regulated by a kinase cascade. To explain the ability of the Pim protein kinases to regulate growth and survival, research has initially focused on the ability of these protein kinases to regulate CDC25A and CDC25C, p21^{Waf1}, and the C-TAK1² protein kinase (12–14). Recently, Pim-1 has been shown to increase the cyclin-dependent kinase-2 activity, by decreasing the levels of p27^{Kip1} (p27) protein (15). Similarly, we have demonstrated that small molecule inhibitors of Pim-1 both translocate the p27 protein to the nucleus and markedly increase its levels (16, 17), suggesting that inhibiting Pim-1 activity may regulate the cell cycle by controlling p27 levels and localization.

The SCF^{Skp2} ubiquitin ligase (Skp1/cullin/F-box protein) targets cell cycle negative regulators p27, p21^{Waf1}, and p130 (18) to the proteasome for degradation and controls progression through the cell cycle. A key protein in this complex Skp2 binds phosphorylated p27 and is responsible for its destruction. The fact that increased Skp2 expression is frequently found in many cancers (19, 20) and Skp2 overexpression can drive cell transformation suggests the importance of the levels of this protein in regulating cell growth (19, 21, 22). The amount of the Skp2 protein in cells is tightly regulated by multiple pathways, including phosphorylation and proteasome degradation. The anaphase-promoting complex or cyclosome (APC/C) is active from mitosis to late G₁ (23, 24) and functions as the E3 ligase for this protein when activated by Cdh1 (25, 26). Phosphorylation of Skp2 by CDK2 (27) and Akt1 (28, 29) on Ser⁶⁴ and Ser⁷² protects it from degradation by the APC/C^{Cdh1} complex and elevates the levels of this protein. However, the role of Skp2 Ser⁷² phosphorylation is under debate as contradictory findings have been reported (30, 31). Further studies are required to elucidate fully the mechanisms by which cells regulate Skp2 levels.

Here, we demonstrate that Pim-1 kinase activity stabilizes and increases the levels of Skp2 protein, thus decreasing p27 levels and promoting cell cycle progression. Pim-1 both binds Skp2 and phosphorylates it on Ser⁶⁴ and Ser⁷², but also on a novel site, Thr⁴¹⁷. Furthermore, Pim-1 phosphorylates Cdh1,

* This work was supported by Department of Defense Grants W81XWH-08 and W81XWH-10-1-0249. The flow cytometry core received support from 1P30-CA138313.

^S The on-line version of this article (available at <http://www.jbc.org>) contains supplemental Figs. S1–S5 and additional references.

¹ To whom correspondence should be addressed: 86 Jonathan Lucas St., Charleston, SC 29425. Fax: 843-792-9456; E-mail: kraft@musc.edu.

² The abbreviations used are: C-TAK1, Cdc25C-associated kinase 1; APC/C, anaphase-promoting complex or cyclosome; HGF, hepatocyte growth factor; SCF, Skp1/cullin/F-box protein.

impairing its association with CDC27 and inhibiting APC/C activity, thus protecting Skp2 from degradation.

EXPERIMENTAL PROCEDURES

Antibodies, Drugs, and Reagents—Anti-Pim-1 (19F7) antibody was produced and purified in this laboratory. Anti-cyclin E (HE12), anti-Met (25H2), anti-phospho-Met (D26), Myc tag (71D10), anti-AKT, anti-phospho-AKT (S473), and anti-polo-like kinase-1 antibodies were purchased from Cell Signaling Technology. Anti-p27 (C19), anti-CDC27 (AF3.1), and anti-cyclin B1 (H-433) were from Santa Cruz Biotechnology. Anti- β -actin (AC-15), anti-FLAG M2, anti-HA (HA-7), and anti- β -tubulin (TUB 2.1) antibodies were from Sigma. Anti-Skp2 and anti-Cks1 antibodies were from Invitrogen/Zymed Laboratories Inc.. Anti-His tag antibody was from Qiagen. Anti-Cdh1(DH01) antibody was from Abcam. Anti-lamin B antibody was from Calbiochem.

Roscovitine and reagents for *in vitro* ubiquitination assay were from Biomol. Cycloheximide, MG132, LY294002, wortmannin, nocodazole, and thymidine were from Sigma. GSK690693 was provided by Glaxo Smith Kline.

Recombinant human HGF was from Antigenix America. Active GST-tagged Pim-1 was from SignalChem. Active His-tagged human Pim-1 was purified from *Escherichia coli* using a Calbiochem nickel-nitrilotriacetic acid column. GST and GST-Skp2 proteins were purified from *E. coli* using glutathione-Sepharose 4B resin (GE Healthcare).

Plasmids—A Pim-1 siRNA plasmid and the control plasmid were described previously (32). pGIPZ Pim-1 shRNA constructs were from Open Biosystems.

pCMV-Skp2 plasmid expressing FLAG-tagged Skp2 was kindly provided by Dr. Liang Zhu (33). Site-directed mutants were prepared using PCR based on this plasmid. HA-Cdh1 and HA-Cdc20 plasmids were described elsewhere (34). The Ubc3 and ubiquitin plasmids have been previously described (35). The HA-Pim-1 and FLAG-Pim-1 constructs were generated by subcloning murine Pim-1 cDNA into pcDNA3 vector, and the K67M (HA-tagged) mutant was constructed using PCR. An N-terminally truncated mutant (NT81) of Pim-1 was described previously (36). Lentiviral expression constructs pLEX-Pim-1 and pLEX-Skp2 was obtained by subcloning human Pim-1 and Skp2 cDNAs into pLEX vector (Open Biosystems). A human Pim-1 construct, pcDNA3-Pim-1, was described elsewhere (32).

Cell Culture, Transfections, Transductions, and Cell Synchronization—Cell lines were grown in RPMI 1640 medium (PC3) or DMEM (HeLa, HEK293T, Rat1, and mouse embryonic fibroblasts). The triple knock-out mouse of the Pim-1, -2, -3 genes used to isolate mouse embryonic fibroblasts were described previously (17). Mouse prostate epithelial cells were isolated as described (37). HEK293T cells were transfected by the calcium phosphate method, and HeLa cells were transfected with Lipofectamine 2000 reagent. Lentiviruses were produced and transduced into Rat1 cells using kits from Open Biosystems.

For synchronization experiments, HeLa cells were treated with 2 mM thymidine for 18 h, washed, and released into fresh medium for 9 h. Then, a second thymidine treatment was

applied to yield cells at the G₁/S transition. Mitotic HeLa cells were obtained by treating HeLa cells with 2 mM thymidine for 24 h, washing, and releasing into fresh medium for 3 h. The cells were then treated with 100 ng/ml nocodazole for 12 h.

Ubiquitination Assays—*In vitro* p27 ubiquitination assays were performed essentially as described (38). In brief, the SCF^{Skp2} complex was expressed and purified from insect cells (39) and mixed with *in vitro*-translated ³⁵S-labeled p27 that had previously been incubated with cyclin E/Cdk2 along with methylated ubiquitin and ubiquitin aldehyde for 60 min at 30 °C. The reaction was stopped with 2× SDS sample buffer and run on polyacrylamide gels. *In vivo* ubiquitination assays were performed as described (40). HEK293T cells were transfected with the indicated plasmids for 24 h, treated with 10 μ M MG132 for 6 h, and lysed in denaturing buffer (6 M guanidine-HCl, 0.1 M Na₂HPO₄/NaH₂PO₄, 10 mM imidazole). The cell extracts were then incubated with nickel beads for 3 h, washed, and subjected to immunoblot analysis.

In Vitro and in Vivo Phosphorylation Assay—FLAG-Skp2 or its mutants were immunoprecipitated with anti-FLAG antibody from HEK293T cells. Immune complexes were washed three times in radioimmune precipitation assay lysis buffer (150 mM NaCl, 10 mM Tris-HCl, pH 7.5, 1% Nonidet P-40, 0.5% deoxycholate, 0.1% SDS), then washed twice in 1× kinase buffer (25 mM Tris-HCl, pH 7.5, 5 mM β -glycerophosphate, 2 mM dithiothreitol, 0.1 mM Na₃VO₄, 10 mM MgCl₂, 2 μ M unlabeled ATP) and incubated with 0.5 μ g of recombinant active Pim-1 kinase and 2 μ Ci of [γ -³²P]ATP in 3 μ l of total reaction buffer for 30 min at 30 °C. Phosphorylation of Cdh1 or Cdc20 was detected using *in vitro* translated proteins produced by TNT Coupled Reticulocyte Lysate System (Promega). Reactions were stopped by washing twice in kinase buffer and boiling in 2× SDS loading buffer. Proteins were resolved by 9% SDS-PAGE, and ³²P incorporation was detected by autoradiography. For *in vivo* labeling experiments, HeLa cells were transfected with the indicated plasmids for 24 h, and the medium was changed to phosphate-free DMEM with 0.5% dialyzed FBS containing 200 μ Ci ml⁻¹ ortho-³²PO₄ for 4 h. Cells were lysed by radioimmune precipitation assay buffer for immunoprecipitation, and the immune complexes were subjected to 9% SDS-PAGE followed by autoradiography analysis.

Flow Cytometry—Cell cycle distribution was monitored by FACS analysis of ethanol-fixed, propidium iodide-stained cells on a Becton Dickinson FACSCalibur Analytical Flow Cytometer.

BrdU Incorporation Assay—Rat1 cells were seeded in 96-well plates (3000 cells/well) and maintained as described in the figure legends. An ELISA BrdU kit (Roche Applied Science) was used to assay the cell cycle. Absorbance at 370 nm (reference wavelength 492 nm) was measured using a Molecular Devices microplate reader.

Densitometry Analysis—Densitometry was determined with ImageJ version 1.42q software (National Institutes of Health) with normalization to the corresponding controls (β -actin or input).

Statistical Analysis—All assays were repeated at least three times. The results of quantitative studies are reported as mean \pm S.D. Differences were analyzed by Student's *t* test. *p* <

Pim-1 Regulates Skp2 Levels

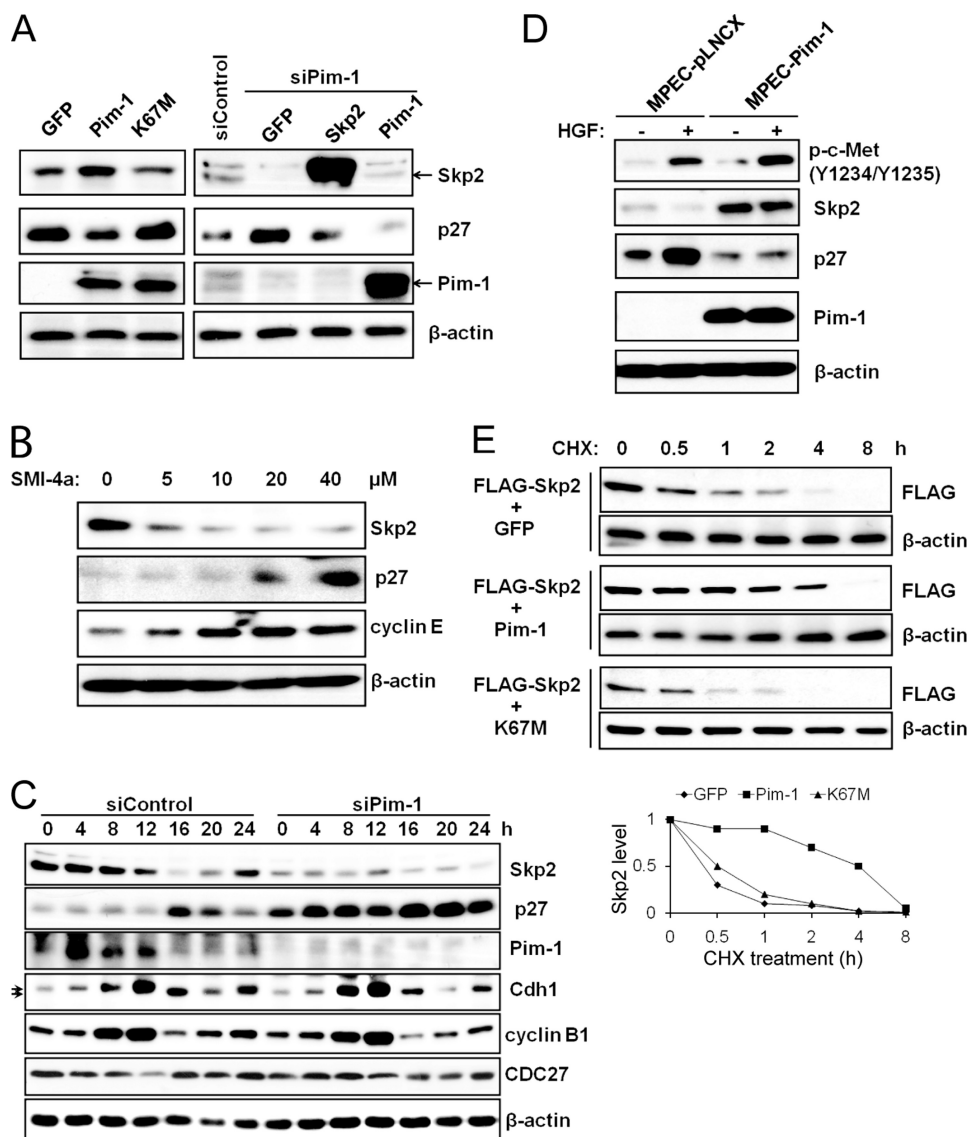


FIGURE 1. Regulation of Skp2 protein levels by Pim-1. *A*, HeLa cells were transiently transfected with cDNAs encoding green fluorescent protein (GFP), Pim-1, kinase-dead Pim-1 (K67M), or a siRNA to Pim-1 together with GFP, or Skp2, or Pim-1, or a scrambled sequence. Forty-eight h after transfection, extracts of these cells were probed on Western blots with the listed antibodies. *B*, HeLa cells were treated with various concentrations of Pim kinase inhibitor SMI-4a for 16 h, extracts were prepared, and immunoblotting was carried out with the identified antibodies. *C*, HeLa cells were transfected with the indicated siRNA plasmids followed by a double-thymidine block treatment (see "Experimental Procedures"). Lysates were prepared at the indicated time points after release from the thymidine block and subjected to immunoblot analysis. Arrows indicate phosphorylated and unphosphorylated forms of Cdh1. *D*, mouse prostate epithelial cells (MPECs) stably transfected with a control vector (pLNCX) or a human Pim-1-expressing plasmid were treated with HGF (50 ng/ml) for 24 h followed by immunoblot analysis. *E*, 24 h after transfection with expression plasmids (time 0), HEK293T cells were incubated for the indicated times with cycloheximide (CHX, 100 μ g/ml) followed by immunoblot analysis with FLAG or β -actin antibodies. Densitometric analysis was performed using ImageJ software to quantify the expression of Skp2. Skp2 band intensity was normalized to β -actin, then normalized to the $t = 0$ controls.

0.05 was regarded as significant, and such differences are indicated in the figures.

RESULTS

Pim-1 Stabilizes Skp2 Protein—Overexpression in HeLa cells of wild type Pim-1 but not a kinase-dead mutant, K67M, leads to a decrease in the level of the p27 protein (Fig. 1A) without any change in the mRNA level of this protein (supplemental Fig. S2D). To evaluate the mechanism by which Pim-1 functions, we focused attention on the E3 ligase SCF complex that

targets p27 for proteasomal degradation and in particular the Skp2 protein which is known to directly bind p27. Western blots demonstrate that transfection of the Pim-1 kinase increases the levels of Skp2 protein (Fig. 1A), while conversely siRNA or shRNA (supplemental Fig. S1A) knockdown of endogenous Pim-1 expression reduces Skp2 levels. The interplay between these two proteins is further demonstrated by the observation that transfection of murine Pim-1 into HeLa cells in which endogenous enzyme has been knocked down again elevates the level of Skp2 (Fig. 1A). Using two small molecule Pim kinase inhibitors, SMI-4a, which has demonstrated excellent selectivity (16, 17, 41), and a structurally unrelated Pim kinase inhibitor, K00135 (27), treatment of both HeLa cells (Fig. 1B) and PC3 prostate cancer cells (supplemental Fig. S1, B and C) causes a dose-dependent reduction of Skp2 protein expression and a concomitant rise in p27. We and others have shown that Pim-1 facilitates cell cycle progression as overexpression of Pim-1 promotes G_1 -S transition (15) whereas Pim kinase inhibitor caused cell cycle arrest at G_1 (16). Because the Akt protein kinase family is thought to control the level of Skp2 (28, 29), we evaluated whether the PI3K inhibitor, wortmannin or a pan-Akt inhibitor, GSK690693, had similar effects on Skp2 levels. However, no significant changes in the levels of Skp2 were seen after treatment with these reagents until the highest concentrations tested (supplemental Fig. S1, D and E). Interestingly, LY294002, which is both a PI3K and Pim-1 inhibitor (9),

reduced Skp2 expression (supplemental Fig. S1E).

To test whether the effects of Pim-1 knockdown were cell cycle-specific, we transfected HeLa cells with Pim-1 siRNA, blocked them in the G_1 /S boundary, and then released them into the cell cycle and measured the Skp2 and p27 levels. We found that the siRNA knockdown of Pim-1 regulated these two proteins throughout the cell cycle (Fig. 1C).

To test the activity of Pim-1 in a different cellular system we examined the role of Pim-1 overexpression in mouse prostate epithelial cells. These cells respond to hepatocyte growth factor

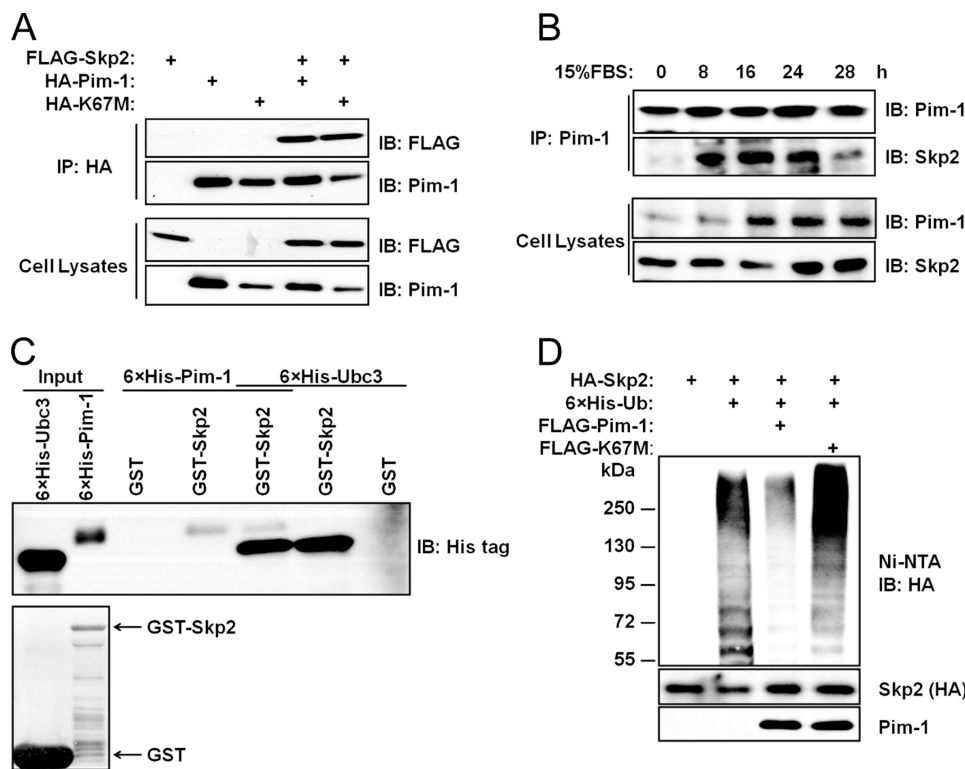


FIGURE 2. Pim-1 binds to Skp2. *A*, HEK293T cells were transfected with the indicated plasmids, protein immunoprecipitated (IP) with HA antibody and immunoblotted with FLAG or Pim-1 antibody. Lysates of cells used for this assay are probed with identical antibodies. *B*, HEK293T cells were serum-starved (0.2%) for 48 h prior to the addition of 15% FBS at 0 time. Cells were then harvested at the indicated time points, and coimmunoprecipitation (co-IP) was performed. *C*, GST-Skp2 proteins were incubated overnight with His-tagged Pim-1 or Ubc3 proteins purified from *E. coli* at 4 °C, washed with PBS, and subjected to immunoblot analysis (upper panel). GST and GST-Skp2 were stained with Coomassie Brilliant Blue (lower panel). *D*, HEK293T cells were transfected with the indicated plasmids, treated with 10 μ M MG132 for 6 h, and ubiquitination as measured by binding to nickel-nitrilotriacetic acid (Ni-NTA) beads (see "Experimental Procedures") followed by an immunoblot with anti-HA antibody. Immunoblot (IB) analysis was performed on total cell lysates from these HEK293T cells (two lower panels).

(HGF), a powerful mitogen and morphogen for epithelial and endothelial cells, through binding to its receptor the Met tyrosine kinase (42, 43). The growth inhibitory activity of HGF on cancer cells is associated with up-regulation of p27 expression (44), mediated by down-regulation of Skp2 expression (45). We found that the HGF-induced p27 up-regulation is inhibited by Pim-1 in mouse prostate epithelial cells (Fig. 1D). Similar results were also obtained in Pim-overexpressing HeLa cells when they were treated with HGF (supplemental Fig. S1F).

Finally, in HEK293T cells the coexpression of Pim-1, but not kinase-dead Pim-1, K67M, or GFP, was able to induce a longer Skp2 half-life (Fig. 1E). Taken together, these experiments suggest that Pim-1 controls the levels of Skp2 and consequently regulates the amounts of p27 protein in cells.

Pim-1 Binds Directly to Skp2 and Reduces Skp2 Ubiquitination—We cotransfected HEK293 cells with FLAG-Skp2 and either HA-Pim-1 or kinase-dead Pim-1 (HA-K67M) expression constructs. When cell lysates were subjected to immunoprecipitation with HA antibody, we found that Pim-1 and Skp2 are able to interact physically in cells irrespective of the Pim-1 kinase activity (Fig. 2A). In HEK293T cells that are transfected then serum-starved and finally released into 15% serum, this interaction between Pim-1 and Skp2 occurs maximally between hours 8 and 24 (Fig. 2B). We did not perform a

cell cycle analysis on these cells. However, knockdown of endogenous Pim-1 in HeLa cells appears to reduce Skp2 expression throughout a full cell cycle (Fig. 1C). These observations suggest that Pim-1 may regulate other molecule(s) controlling Skp2 levels *in vivo*. This binding is also seen *in vitro* in glutathione *S*-transferase (GST) pull-down experiments. Recombinant His-tagged Pim-1 protein binds to Skp2; the binding of Pim-1 did not interfere with the interaction between Skp2 and Ubc3, an E2 ubiquitin enzyme that is known to interact with the Skp2 protein (Fig. 2C). Furthermore, Pim-1 did not interfere with the formation of the SCF^{Skp2} complex, from Skp2, Ubc3, and Rbx1 proteins (supplemental Fig. S2A).

Like p27, Skp2 levels are regulated by ubiquitination and proteasome degradation (25, 26), suggesting that Pim-1 could decrease the levels of Skp2 ubiquitination. Using protein extracts from HEK293T cells transfected with Pim-1 and Skp2, we found that the presence of active but not kinase-dead Pim-1 is sufficient to repress the ubiquitination of the Skp2 protein markedly (Fig. 2D). Using this same approach,

consistent with the effect on Skp2, Pim-1 transfection was found to also increase p27 ubiquitination (supplemental Fig. S2C). This suggests that an increase in Skp2 levels is needed to mediate increased ubiquitination of p27 by Pim-1. Indeed, in an *in vitro* assay, the presence of Pim-1 did not directly influence p27 ubiquitination (supplemental Fig. S2B).

Pim-1 Phosphorylates Skp2 on Multiple Sites—To determine whether Skp2 was a substrate for Pim-1, purified His-tagged protein kinase was incubated with immunoprecipitated FLAG-Skp2 in the presence of [γ -³²P]ATP. In this assay, Skp2 was clearly phosphorylated, and this phosphorylation was decreased by the addition of a small molecule Pim-1 inhibitor, SMI-4a (Fig. 3A). Pim-1 is known to phosphorylate the sequence R-X-R-L-S/T (46). Scanning the Skp2 sequence, we identified a potential Pim-1 consensus site at the C terminus of Skp2, Thr⁴¹⁷, which is conserved from frog to humans (Fig. 3B). Mutation of this residue from threonine to alanine (T417A) led to reduced Skp2 phosphorylation by Pim-1 *in vitro*, but did not completely abolish this modification (Fig. 3C). Previous studies (8–10) have demonstrated that Ser⁶⁴ and Ser⁷² in Skp2 are CDK2 phosphorylation sites (27), and Ser⁷² can also be phosphorylated by Akt1 (28, 29). Using GST-Pim-1 as a kinase, mutation of either Ser⁶⁴ or Ser⁷² to Ala markedly decreased Skp2 phosphorylation by Pim-1 with both of these changes hav-

Pim-1 Regulates Skp2 Levels

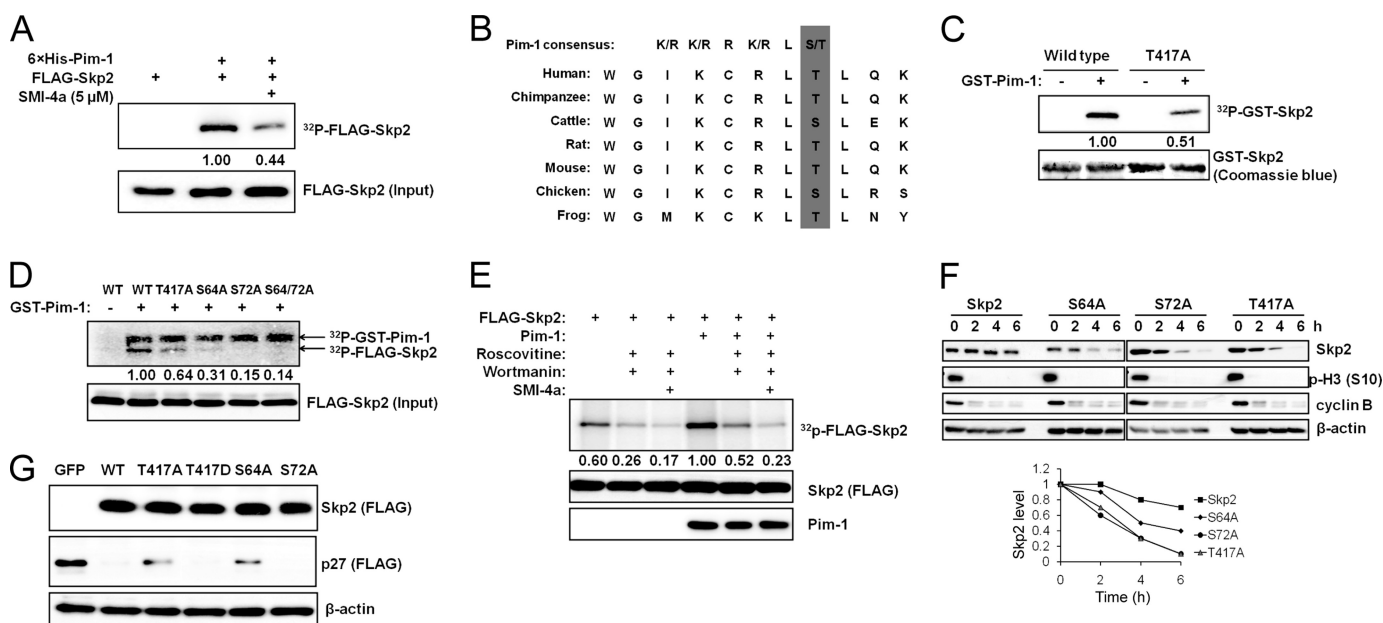


FIGURE 3. Pim-1 phosphorylates Skp2. **A**, FLAG-Skp2 was immunoprecipitated from HEK293T cells, incubated with recombinant His-tagged Pim-1 for 30 min with or without SMI-4a for an *in vitro* kinase assay ("Experimental Procedures") followed by SDS-PAGE autoradiography (*upper panel*) and immunoblot analyses (*lower panel*). The phosphorylation of FLAG-Skp2 was quantified by densitometry from three independent experiments after normalization to input. **B**, C-terminal sequence of Skp2 contains a Pim-1 consensus site. **C**, GST-tagged Skp2 proteins or a T417A mutant was incubated with recombinant GST-Pim-1 and [γ - 32 P]ATP for 30 min, and subjected to SDS-PAGE followed by autoradiography. The phosphorylation of GST-Skp2 was quantified by densitometry from three independent experiments with normalization to Coomassie Blue staining. **D**, wild type (WT) FLAG-Skp2 and its mutants T417A, S64A, S72A, and S64A/S72A were immunoprecipitated from HEK293T cells, incubated with recombinant GST-tagged Pim-1 and [γ - 32 P]ATP for 30 min, followed by SDS-PAGE autoradiography (*upper panel*) and immunoblot analysis (*lower panel*). The phosphorylation of FLAG-Skp2 was quantified by densitometry from three independent experiments following normalization to the level of protein input. **E**, HeLa cells were pretreated with roscovitine (20 μ M), wortmannin (1 μ M), or SMI-4a (10 μ M) for 1 h, transfected with human Pim-1 and Skp2, and labeled with 32 P_i followed by FLAG immunoprecipitation, autoradiography (*upper panel*), and FLAG/Pim-1 immunoblots (*two lower panels*). The phosphorylation of FLAG-Skp2 was quantified by densitometry from three independent experiments along with normalization to Skp2 expression. **F**, HeLa cells were transfected with the indicated Skp2 constructs and synchronized in M phase by mitotic shake-off of cells obtained after release from a thymidine-nocodazole block. The cells were then replated and allowed to progress through the cell cycle in the presence of cycloheximide (100 μ g/ml). Immunoblot analysis was performed at specific time points using antibodies to cyclin B and phosphohistone H3 Ser¹⁰ (*p-H3* (S10)) as controls. Densitometric analysis was performed using ImageJ software to quantify the expression of Skp2. Skp2 band intensity was normalized to β -actin and then normalized to the $t = 0$ controls. **G**, HEK293T cells were transfected with a FLAG-tagged p27 Skp2 construct or a GFP control. Expression of exogenous p27 and Skp2 is measured by immunoblotting.

ing a somewhat greater effect than the T417A mutation (Fig. 3D), suggesting that each of these sites might also be a Pim-1 target. It appears that phosphorylation of Ser⁶⁴ and/or Ser⁷² may be required for Thr⁴¹⁷ phosphorylation to take place because mutation of either Ser⁶⁴ or Ser⁷² almost completely abolished Skp2 phosphorylation in this experiment. However, a complete understanding of the relationship between these sites requires further studies.

To test whether Pim-1 has a role in regulating Skp2 phosphorylation *in vivo*, HeLa cells were transfected with Pim-1 and Skp2, metabolically labeled with orthophosphate, and then treated with kinase inhibitors such as roscovitine (pan-CDK inhibitor), wortmannin (PI3K inhibitor), and SMI-4a (Pim-1 inhibitor). Treatment with roscovitine and wortmannin reduced Skp2 phosphorylation *in vivo*. Overexpression of Pim-1 markedly increased Skp2 phosphorylation, and this phosphorylation was inhibited by all three agents (Fig. 3E), suggesting that multiple kinases can play a role in regulating phosphorylation of this protein.

Skp2 is degraded by the APC/C^{Cdh1} (25, 26) which is known to have its highest activity from late mitosis to the G₁ phase of the cell cycle (47). To test the impact of phosphorylation of Skp2 on protein stability, we used HeLa cells that were released from a thymidine-nocodazole block in the G₁ phase of the cell

cycle into media containing cycloheximide. Exit from mitosis was monitored by the loss of histone H3 phospho-Ser¹⁰ immunoreactivity and the degradation of cyclin B1 on Western blots (Fig. 3F). Using this technique, we found that all three individual Skp2 phosphorylation mutants were more efficiently degraded than the wild type Skp2 protein (Fig. 3F), suggesting that phosphorylation by protein kinases, including Pim-1, controls the rate of degradation of Skp2.

We next examined the biological activity of wild type and Skp2 phosphorylation mutants by transfecting them along with p27 into HeLa cells and then examining p27 levels by Western blotting. We found that both the Skp2 T417A and S64A mutants decreased the ability of Skp2 to stimulate the degradation of p27, but T417A retained some degrading activity (Fig. 3G). In contrast, an aspartate mutation, T417D, that mimics phosphorylation at this site was more efficient than the T417A at degrading p27. Surprisingly, S72A mutation did not cause any detectable effect on p27 degradation (Fig. 3G).

Pim-1 Impairs Cdh1 and CDC27 Interaction and Phosphorylates Cdh1—Because Pim-1 regulates Skp2 ubiquitination, we examined whether this enzyme might interact with components of the APC/C complex that are responsible for Skp2 degradation. In coimmunoprecipitation experiments done in transfected HEK293T cells, Pim-1 was found to complex with

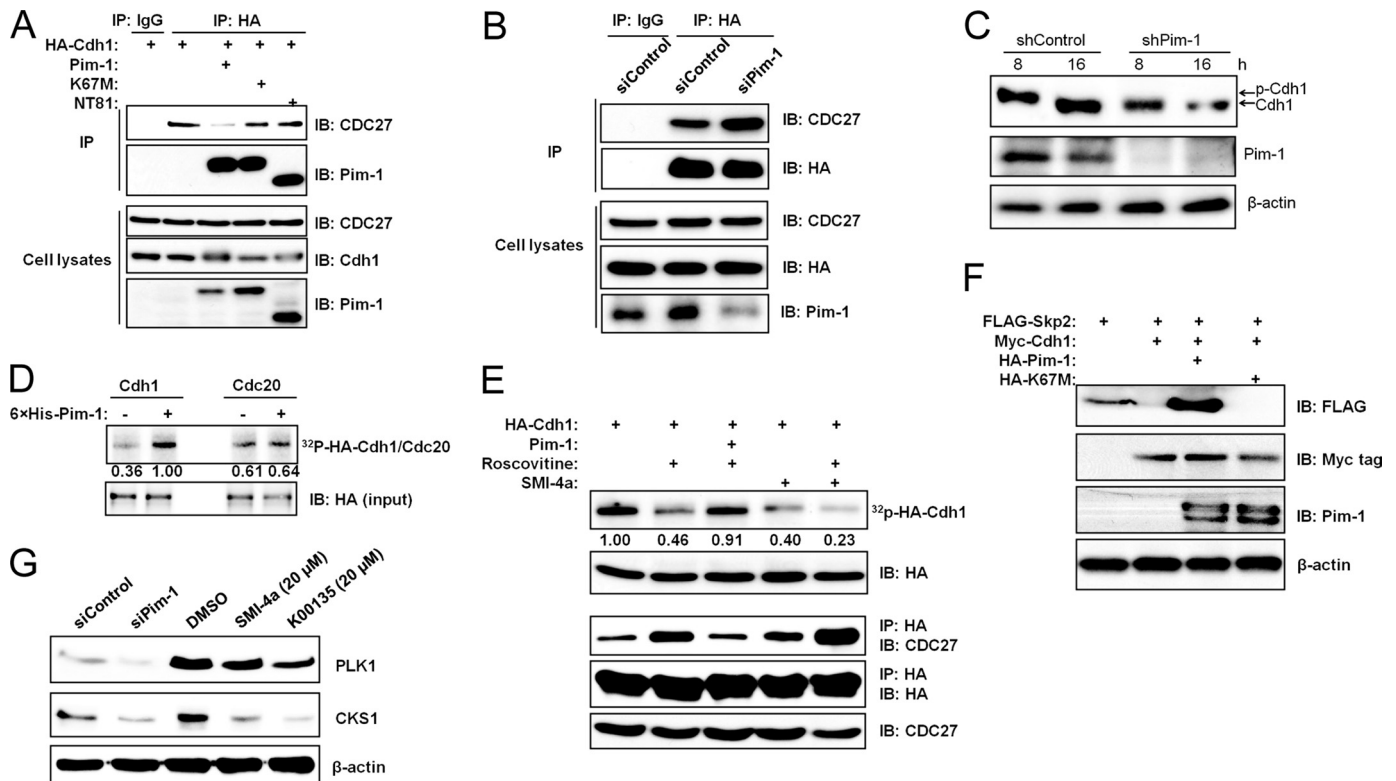


FIGURE 4. Pim-1 kinase phosphorylates Cdh1 and impairs its binding to CDC27. *A*, HEK293T cells were transfected with HA-Cdh1, Pim-1, or kinase-dead Pim-1 K67M or NT81, immunoprecipitated (IP) with HA antibody followed by Western blotting with antibodies to CDC27 and Pim-1. Lysates from these cells were immunoblotted (IB) with antibody as shown. *B*, HeLa cells were cotransfected with HA-Cdh1 and Pim-1 or scrambled siRNA plasmids before harvesting for coimmunoprecipitation analysis. Levels of transfected proteins in lysates were monitored by immunoblotting. *C*, HeLa cells were transfected with the indicated shRNA plasmids followed by a double-thymidine block. After release from the block cell, lysates were prepared at 8 and 16 h and subjected to immunoblot analysis. The arrows indicate phosphorylated and unphosphorylated Cdh1. *D*, *in vitro* translated HA-tagged Cdh1 or Cdc20 was incubated with recombinant Pim-1 and [γ -³²P]ATP in an *in vitro* kinase assay. Autoradiography (upper panel) and immunoblot (lower panel) analyses were performed. The phosphorylation of Cdh1 or Cdc20 was quantified by densitometry from three independent experiments after normalization to the loaded protein. *E*, HeLa cells were transfected with HA-Cdh1 and human Pim-1, and the kinase inhibitors roscovitine (20 μ M) and SMI-4a (10 μ M) were added 1 h before labeling with ³²P_i. HA-Cdh1 was immunoprecipitated, and autoradiography (top panel) and immunoblot analysis were performed (second panel). The phosphorylation of Cdh1 was quantified by densitometry from three independent experiments with normalization to Cdh1 expression (HA). A coimmunoprecipitation experiment was performed to monitor Cdh1 and CDC27 interaction under the same experimental conditions (lower three panels). *F*, HEK293T cells were transfected with FLAG-Skp2, myc-Cdh1, and HA-tagged WT and kinase-dead (K67M) Pim1 kinase, and the extracts were immunoblotted with the specified antibodies. *G*, HeLa cells were transiently transfected with a siRNA to Pim-1 or a scrambled sequence. Forty-eight h after transfection, extracts of these cells were probed on Western blots with the listed antibodies (left two lanes). HeLa cells were treated with 20 μ M Pim kinase inhibitor SMI-4a or K00135 for 16 h, extracts were prepared, and immunoblotting was carried out with the identified antibodies (right three lanes).

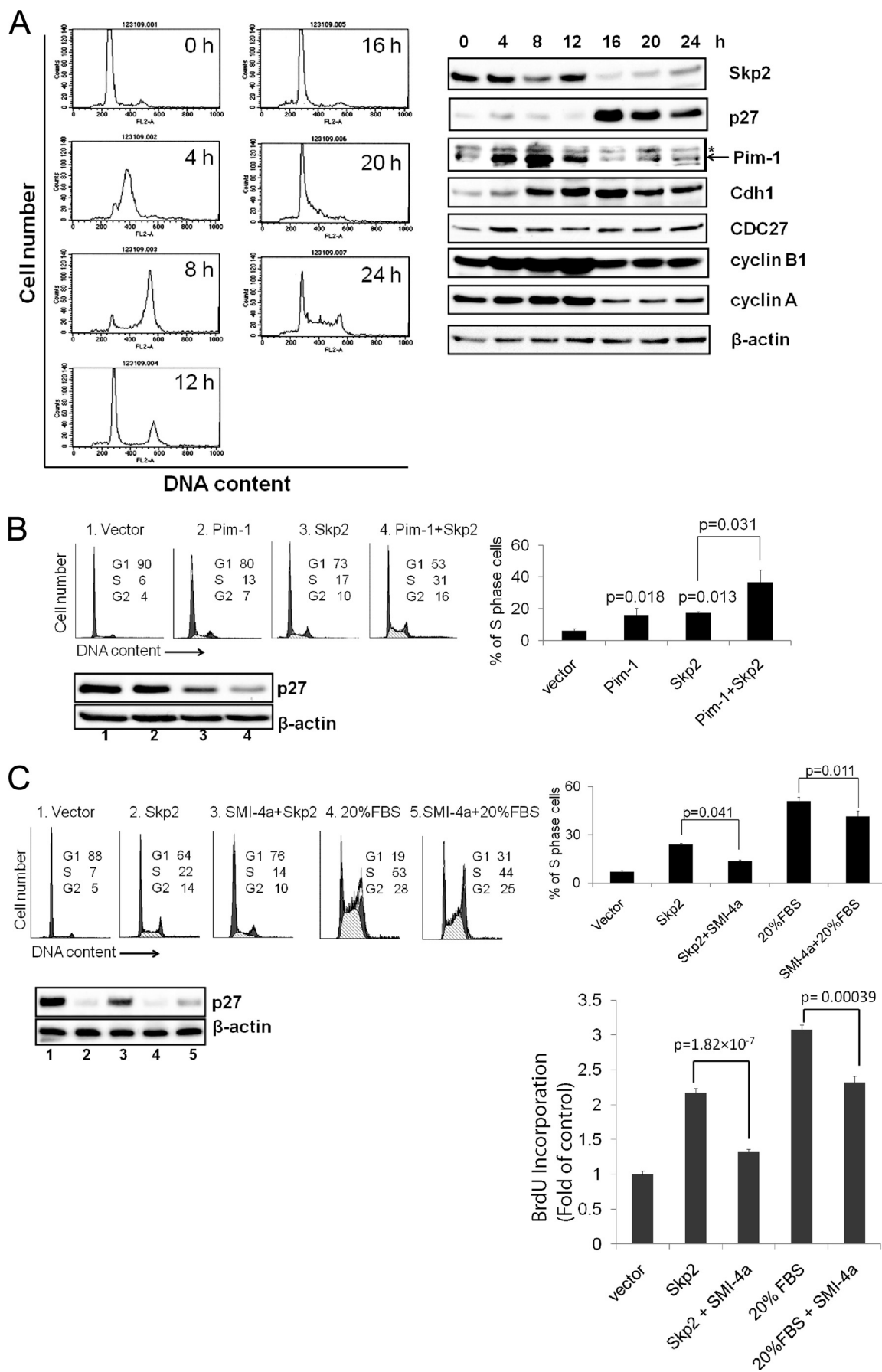
either Cdh1 or CDC20, two well known activators of APC/C (supplemental Fig. S3A). However, Pim-1 did not physically impair the interaction between Cdh1 or CDC20 and Skp2 (supplemental Fig. S3B). Using the same methodology, in contrast, we found that Pim-1 could impair the interaction between Cdh1 and CDC27, another APC/C component, in a phosphorylation-dependent manner (Fig. 4A). The two kinase-dead Pim-1 mutants, K67M and NT81 (36), are also able to form a complex with Cdh1, but only wild type Pim-1 was capable of reducing the interaction between Cdh1 and CDC27 (Fig. 4A). Additionally, incubation with the Pim-1 inhibitor, SMI-4a (supplemental Fig. S4C) or treatment with siRNA to knock down endogenous Pim-1 expression (Fig. 4B) increased the Cdh1/CDC27 interaction.

Our results are consistent with previous findings that demonstrate that phosphorylation of Cdh1 dissociates this protein from the APC/C complex (48, 49). Cdh1 is hyperphosphorylated *in vivo* during S, G₂, and M phases, and this phosphorylation causes an electrophoretic mobility shift on SDS-polyacrylamide gels (Fig. 5A) (48, 50, 51). To explore the role of

Pim-1 in phosphorylation of Cdh1 further, we first reprobbed the same membrane used in Fig. 1C with antibodies against Cdh1 and CDC27. In cells treated with Pim-1 siRNA, Cdh1 displayed higher mobility at 0, 4, 8, and 12 h compared with those in control cells (Fig. 1C), suggesting that phosphorylation was reduced. To confirm this finding, we knocked down endogenous Pim-1 expression in HeLa cells using shRNA and then subjected these cells to a double-thymidine block. The cells were then released from the block (for cell cycle analysis, see Fig. 5A), and immunoblotting was performed to examine Cdh1 phosphorylation. Phosphorylation of endogenous Cdh1 at 8 h after release from a double-thymidine block was dramatically reduced in Pim-1 knockdown cells as judged by the protein mobility shift (Fig. 4C).

Additionally, we found that recombinant Pim-1 was capable of phosphorylating *in vitro* translated Cdh1 but not CDC20 (Fig. 4D). Cdh1 is heavily phosphorylated by CDKs *in vivo*. To examine whether Pim-1 can also phosphorylate Cdh1 *in vivo*, we first treated HeLa cells with the CDK inhibitor roscovitine or Pim inhibitor SMI-4a and then labeled them with ³²P_i.

Pim-1 Regulates Skp2 Levels



Roscovitin or SMI-4a treatment reduced Cdh1 phosphorylation, and overexpression of Pim-1 in the presence of roscovitin reversed the roscovitin effect, although the combination of roscovitin and SMI-4a treatment further decreased Cdh1 phosphorylation (Fig. 4E). We performed coimmunoprecipitation experiments to monitor the Cdh1/CDC27 interactions under these conditions. Consistently, roscovitin treatment increased the Cdh1/CDC27 interaction whereas overexpression of Pim-1 in the presence of roscovitin suppressed this effect. Combined treatment with roscovitin and SMI-4a further increased the Cdh1/CDC27 interaction compared with roscovitin or SMI-4a alone (Fig. 4E).

Because the APC/C activity to degrade Skp2 can be activated by Cdh1 overexpression (25, 26), we tested the ability of Pim-1 to reverse this effect. We found that coexpression of wild-type Pim-1, but not its mutant, K67M, is capable of blocking Cdh1-mediated degradation of Skp2 (Fig. 4F). However, data in Fig. 4F cannot distinguish whether Pim-1 blocks degradation of Skp2 by acting on Cdh1 or Skp2 or both.

Because Pim-1 expression impairs APC/C^{Cdh1} activity, we examined whether other known APC/C^{Cdh1} substrates are regulated by Pim-1 expression. Knockdown of endogenous Pim-1 expression or suppression of Pim-1 kinase activity with Pim kinase inhibitors SMI-4a or K00135 in HeLa cells led to reduced protein expression of both polo-like kinase-1 and CDK subunit 1 (Cks1), two proteins known to be regulated by APC/C^{Cdh1} (Fig. 4G). This finding further demonstrates that Pim-1 is a negative regulator of APC/C^{Cdh1} activity.

Pim-1 Is Required for Skp2 to Signal Cell Cycle S Phase Entry—Based on the activities of Pim-1, we have attempted to correlate the levels of this enzyme with other cell cycle regulatory components. HeLa cells were released from a double-thymidine block, cell cycle progression was monitored by FACS analysis (Fig. 5A), and the expression patterns of Skp2, p27, Cdh1, CDC27, cyclin B1, and cyclin A were measured by Western blotting (Fig. 5B). We found that Pim-1 levels were very high at S (4 h) and G₂/M phases (8 h) of the cell cycle. Lower Pim-1 expression was seen at G₁ and the G₁/S boundary (0, 16, 20, and 24 h; Figs. 5A and 1C). Because Pim-1 is a constitutively active kinase (7–11), this expression pattern of Pim-1 should represent its activity profile during cell cycle progression. Interestingly, but not surprisingly, Pim-1 activity coincides with Skp2 expression (Fig. 5A) and inversely correlates with Cdh1 activity (47, 52) during the cell cycle (Fig. 5A). Because Skp2 is known to have the ability to induce S phase in quiescent fibroblasts (40, 53), we determined whether the Skp2/Pim-1 interaction is important for S phase progression. Investigation of this question was carried out using Rat1 cells because they were able to undergo complete cell cycle blockade at G₀/G₁ upon serum starvation. As judged by FACS analysis, we found that in the absence of serum addition, overexpressed Skp2 or Pim-1 each stimulates S phase entry (Fig. 5B), and coexpression of Skp2 and

Pim-1 further enhances the S phase entry of these cells (Fig. 5B). Conversely, as revealed by both FACS analysis and BrdU incorporation, treatment with a small molecule Pim inhibitor, SMI-4a, reduced Skp2-induced S phase progression (Fig. 5C) and impaired serum-induced S phase entry (Fig. 5C). Another structurally unrelated small molecule Pim inhibitor, K00135 (54), displayed a similar effect (supplemental Fig. S5A). These observations suggest that Pim kinases are required along with Skp2 to allow cells to exit from quiescence.

DISCUSSION

The data presented suggest the novel observation that the Pim-1 protein kinase through a dual mechanism can regulate the levels and hence the activity of Skp2. Pim-1 is capable of binding and phosphorylating Skp2 and stabilizing protein levels, but does not affect the interaction of Skp2 with the E2 ligase Ubc3. Conversely, both siRNA and small molecule Pim-1 inhibitors decrease Skp2 levels and phosphorylation. Skp2 is phosphorylated by CDK2 at Ser⁶⁴ and Ser⁷² (27) and by Akt1 at Ser⁷² to stabilize this protein (28, 29). Pim-1 appears capable of phosphorylating Skp2 at these two sites (Fig. 3), as well as a unique site in the C terminus, Thr⁴¹⁷, that is highly conserved throughout the animal kingdom, including humans and mice. Phosphorylation of this site is required for maximal Skp2 activity and stabilization of Skp2 protein levels *in vivo* (Fig. 3). In the prostate cancer cell line PC3 that contains an activated Akt, a small molecule Pim inhibitor SMI-4a but not wortmannin or the Akt inhibitor GSK690693 decreased the levels of Skp2. LY294002, which inhibits both Akt and Pim, displayed an effect similar to that of SMI-4a, suggesting that in this cell line the Pims are essential for the regulation of Skp2 levels. Unlike Akt (28, 29), Pim-1 kinase did not appear to regulate Skp2 subcellular localization (supplemental Fig. S4). The Pim kinases share multiple similarities with AKT (1, 55, 56). It is possible that the relative abundance of each of these Skp2-phosphorylating kinases may decide which is essential to the control of Skp2 levels. It is quite surprising that our Skp2 S72A mutant did not lose p27 degradation activity compared with the wild type Skp2 (Fig. 3G) because two previous studies demonstrated that this very same Skp2 mutant completely lost ubiquitin ligase activity (28, 29). However, another two recent reports confirmed our finding (30, 31). The half-life of this mutant was indeed shorter than that of wild-type Skp2 (Fig. 3F), consistent with previous reports (27–29).

The degradation of Skp2 is regulated by APC/C^{Cdh1} complex (25, 26) which preferentially associates with non-phospho-Ser⁶⁴ form of Skp2 (27). Pim-1 kinase activity does not affect the binding of Cdh1 to total Skp2 (supplemental Fig. S3B), but does impair the interaction between Cdh1 and CDC27 (Fig. 4A). Interaction with CDC27/APC3 protein allows Cdh1 to activate the APC/C (57). Although Cdh1 is inhibited by both the Emi-1 protein and multiple phosphorylations initiated in part by

FIGURE 5. Pim-1 is required for Skp2 to signal cell cycle S phase entry. A, HeLa cells were treated with a double-thymidine block and released into fresh medium. Cells were then harvested at the indicated time points and subjected to FACS (left panel) and immunoblot analysis (right panel). The arrow denotes the Pim-1 signal. * indicates a nonspecific signal. B, Rat1 cells were transduced with a lentivirus carrying the indicated cDNAs. Cells were maintained in low serum conditions (0.2%) for 48 h before harvested for FACS (upper panel) and immunoblot (lower panel) analyses. Percent of S phase cells was compared with vector control, except where indicated by a bracket. C, the experiment was performed as in B except that SMI-4a (5 μM) was added 3 h before a 20% FBS stimulation (16 h). S phase induction was also determined by BrdU incorporation assay. Brackets indicate comparison of with and without SMI-4a treatment.

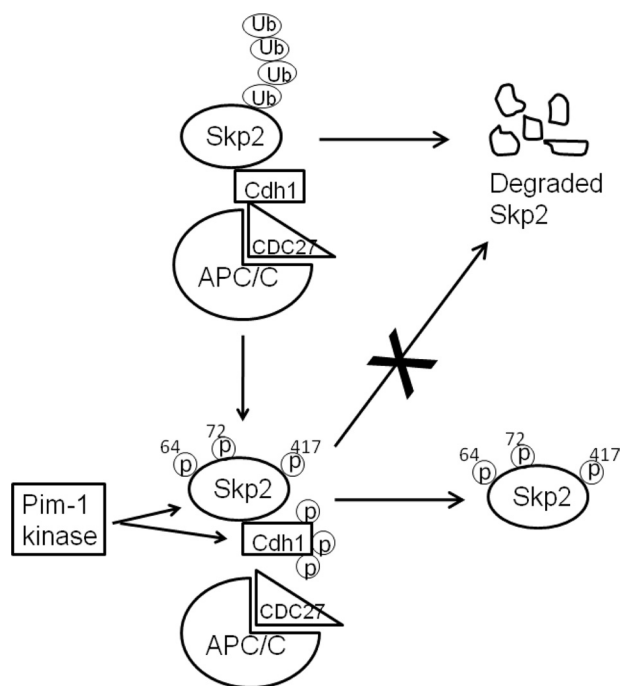


FIGURE 6. Model of Pim-1 regulation on Skp2 degradation. Nonphosphorylated Skp2 binds to E3 ligase APC/C^{Cdh1} and gets ubiquitinated (Ub) followed by proteasome-mediated degradation. Pim-1 kinase phosphorylates Skp2 on multiple sites: Ser⁶⁴, Ser⁷², and Thr⁴¹⁷. Furthermore, the phosphorylation of Cdh1 by Pim-1 reduces Cdh1 and APC/C interaction. Both Pim-1 actions result in decreased Skp2 ubiquitination and consequently increased Skp2 stability.

cyclin A-CDK2 and cyclin B1-CDK1 (47, 52), it has been proposed that an additional kinase may play a role (58). Here, we demonstrate that Cdh1 is a phosphorylation target of Pim-1 (Fig. 4, D and E) and the knockdown of Pim-1 with siRNA reduces Cdh1 phosphorylation during S, G₂, and M phases (Figs. 1C and 4C), demonstrating the critical involvement of Pim-1 in tightly controlled Cdh1 phosphorylation during the cell cycle. It remains unknown whether Pim-1 and CDKs share some phosphorylation sites on Cdh1. Further studies are required to determine the precise Pim-1 sites and how these two different types of kinases cooperate to control Cdh1 activity. Interestingly, the levels of Pim-1 protein are correlated with Cdh1 phosphorylation during cell cycle progression as high Pim-1 expression and high Cdh1 phosphorylation were seen during S, G₂, and M phases, and the opposite occurred during the G₁ phase (Fig. 5A). Given the role of Cdh1 in regulating mitosis, this may explain why Pim-1 is not only required for Skp2 to signal S phase entry (Fig. 5), but also plays a critical role in G₂/M phase regulation. Consistent with this hypothesis, mouse embryo fibroblasts that are knocked out for all three Pim kinase isoforms display increased number of cells in the G₂/M phase of the cell cycle (supplemental Fig. S5). These observations are in concert with previous discoveries suggesting that Pim-1 functions in mitosis (59–61). Therefore, the Pim-1 kinase regulates Skp2 levels through the Pim-1 kinase activity, reduces APC/C^{Cdh1} E3 ligase activity, and thus protects Skp2 from degradation (Fig. 4F).

The Pim-1 protein kinase is abnormally elevated in human cancers, regulated by growth factors, and collaborates with other oncogenes to induce cell transformation (1, 2, 5, 6). The

ability of this enzyme to modulate the activity of both the SCF^{Skp2} and APC/C^{Cdh1} (Fig. 6) and thus control p27 levels is likely to be essential to the biological activities of this protein kinase.

Acknowledgments—We thank Dr. Liang Zhu (Albert Einstein College of Medicine, Yeshiva University) for providing the Skp2 expression construct and Dr. Xuedong Liu (University of Colorado-Boulder) for providing the active Skp2 complex for the in vitro ubiquitination assay.

REFERENCES

1. Hammerman, P. S., Fox, C. J., Birnbaum, M. J., and Thompson, C. B. (2005) *Blood* **105**, 4477–4483
2. Ellwood-Yen, K., Graeber, T. G., Wongvipat, J., Iruela-Arispe, M. L., Zhang, J., Matusik, R., Thomas, G. V., and Sawyers, C. L. (2003) *Cancer Cell* **4**, 223–238
3. Zippo, A., De Robertis, A., Serafini, R., and Oliviero, S. (2007) *Nat. Cell Biol.* **9**, 932–944
4. Dhanasekaran, S. M., Barrette, T. R., Ghosh, D., Shah, R., Varambally, S., Kurachi, K., Pienta, K. J., Rubin, M. A., and Chinnaiyan, A. M. (2001) *Nature* **412**, 822–826
5. Shah, N., Pang, B., Yeoh, K. G., Thorn, S., Chen, C. S., Lilly, M. B., and Salto-Tellez, M. (2008) *Eur. J. Cancer* **44**, 2144–2151
6. Speers, C., Tsimelzon, A., Sexton, K., Herrick, A. M., Gutierrez, C., Culhane, A., Quackenbush, J., Hilsenbeck, S., Chang, J., and Brown, P. (2009) *Clin. Cancer Res.* **15**, 6327–6340
7. Bullock, A. N., Debreczeni, J., Amos, A. L., Knapp, S., and Turk, B. E. (2005) *J. Biol. Chem.* **280**, 41675–41682
8. Kumar, A., Mandiyan, V., Suzuki, Y., Zhang, C., Rice, J., Tsai, J., Artis, D. R., Ibrahim, P., and Bremer, R. (2005) *J. Mol. Biol.* **348**, 183–193
9. Jacobs, M. D., Black, J., Futer, O., Swenson, L., Hare, B., Fleming, M., and Saxena, K. (2005) *J. Biol. Chem.* **280**, 13728–13734
10. Qian, K. C., Wang, L., Hickey, E. R., Studts, J., Barringer, K., Peng, C., Kronkatis, A., Li, J., White, A., Mische, S., and Farmer, B. (2005) *J. Biol. Chem.* **280**, 6130–6137
11. Bullock, A. N., Russo, S., Amos, A., Pagano, N., Bregman, H., Debreczeni, J. E., Lee, W. H., von Delft, F., Meggers, E., and Knapp, S. (2009) *PLoS One* **4**, e7112
12. Mochizuki, T., Kitanaka, C., Noguchi, K., Muramatsu, T., Asai, A., and Kuchino, Y. (1999) *J. Biol. Chem.* **274**, 18659–18666
13. Bachmann, M., Hennemann, H., Xing, P. X., Hoffmann, I., and Möroy, T. (2004) *J. Biol. Chem.* **279**, 48319–48328
14. Wang, Z., Bhattacharya, N., Mixter, P. F., Wei, W., Sedivy, J., and Magnuson, N. S. (2002) *Biochim. Biophys. Acta* **1593**, 45–55
15. Morishita, D., Katayama, R., Sekimizu, K., Tsuruo, T., and Fujita, N. (2008) *Cancer Res.* **68**, 5076–5085
16. Beharry, Z., Zemska, M., Mahajan, S., Zhang, F., Ma, J., Xia, Z., Lilly, M., Smith, C. D., and Kraft, A. S. (2009) *Mol. Cancer Ther.* **8**, 1473–1483
17. Lin, Y. W., Beharry, Z. M., Hill, E. G., Song, J. H., Wang, W., Xia, Z., Zhang, Z., Aplan, P. D., Aster, J. C., Smith, C. D., and Kraft, A. S. (2009) *Blood* **115**, 824–833
18. Cardozo, T., and Pagano, M. (2004) *Nat. Rev. Mol. Cell Biol.* **5**, 739–751
19. Gstaiger, M., Jordan, R., Lim, M., Catzavelos, C., Mestan, J., Slingerland, J., and Krek, W. (2001) *Proc. Natl. Acad. Sci. U.S.A.* **98**, 5043–5048
20. Signoretti, S., Di Marcotullio, L., Richardson, A., Ramaswamy, S., Isaac, B., Rue, M., Monti, F., Loda, M., and Pagano, M. (2002) *J. Clin. Invest.* **110**, 633–641
21. Latres, E., Chiarle, R., Schulman, B. A., Pavletich, N. P., Pellicer, A., Inghirami, G., and Pagano, M. (2001) *Proc. Natl. Acad. Sci. U.S.A.* **98**, 2515–2520
22. Shim, E. H., Johnson, L., Noh, H. L., Kim, Y. J., Sun, H., Zeiss, C., and Zhang, H. (2003) *Cancer Res.* **63**, 1583–1588
23. Reed, S. I. (2003) *Nat. Rev. Mol. Cell Biol.* **4**, 855–864
24. Nakayama, K. I., and Nakayama, K. (2006) *Nat. Rev. Cancer* **6**, 369–381

25. Bashir, T., Dorrello, N. V., Amador, V., Guardavaccaro, D., and Pagano, M. (2004) *Nature* **428**, 190–193
26. Wei, W., Ayad, N. G., Wan, Y., Zhang, G. J., Kirschner, M. W., and Kaelin, W. G., Jr. (2004) *Nature* **428**, 194–198
27. Rodier, G., Coulombe, P., Tanguay, P. L., Boutonnet, C., and Meloche, S. (2008) *EMBO J.* **27**, 679–691
28. Gao, D., Inuzuka, H., Tseng, A., Chin, R. Y., Toker, A., and Wei, W. (2009) *Nat. Cell Biol.* **11**, 397–408
29. Lin, H. K., Wang, G., Chen, Z., Teruya-Feldstein, J., Liu, Y., Chan, C. H., Yang, W. L., Erdjument-Bromage, H., Nakayama, K. I., Nimer, S., Tempst, P., and Pandolfi, P. P. (2009) *Nat. Cell Biol.* **11**, 420–432
30. Bashir, T., Pagan, J. K., Busino, L., and Pagano, M. (2010) *Cell Cycle* **9**, 971–974
31. Boutonnet, C., Tanguay, P. L., Julien, C., Rodier, G., Coulombe, P., and Meloche, S. (2010) *Cell Cycle* **9**, 975–979
32. Zemska, M., Sahakian, E., Bashkurova, S., and Lilly, M. (2008) *J. Biol. Chem.* **283**, 20635–20644
33. Ji, P., Jiang, H., Rekhman, K., Bloom, J., Ichetovkin, M., Pagano, M., and Zhu, L. (2004) *Mol. Cell* **16**, 47–58
34. Biggs, J. R., Peterson, L. F., Zhang, Y., Kraft, A. S., and Zhang, D. E. (2006) *Mol. Cell Biol.* **26**, 7420–7429
35. Cen, B., Li, H., and Weinstein, I. B. (2009) *J. Biol. Chem.* **284**, 5265–5276
36. Aho, T. L., Sandholm, J., Peltola, K. J., Mankonen, H. P., Lilly, M., and Koskinen, P. J. (2004) *FEBS Lett.* **571**, 43–49
37. Barclay, W. W., and Cramer, S. D. (2005) *Prostate* **63**, 291–298
38. Carrano, A. C., Eytan, E., Hershko, A., and Pagano, M. (1999) *Nat. Cell Biol.* **1**, 193–199
39. Wang, W., Ungermannova, D., Chen, L., and Liu, X. (2003) *J. Biol. Chem.* **278**, 32390–32396
40. Kim, S. Y., Herbst, A., Tworkowski, K. A., Salghetti, S. E., and Tansey, W. P. (2003) *Mol. Cell* **11**, 1177–1188
41. Xia, Z., Knaak, C., Ma, J., Beharry, Z. M., McInnes, C., Wang, W., Kraft, A. S., and Smith, C. D. (2009) *J. Med. Chem.* **52**, 74–86
42. Balkovetz, D. F., and Lipschutz, J. H. (1999) *Int. Rev. Cytol.* **186**, 225–260
43. Bottaro, D. P., Rubin, J. S., Faletto, D. L., Chan, A. M., Kmiecik, T. E., Vande Woude, G. F., and Aaronson, S. A. (1991) *Science* **251**, 802–804
44. Nagahara, H., Vocero-Akbani, A. M., Snyder, E. L., Ho, A., Latham, D. G., Lissy, N. A., Becker-Hapak, M., Ezhevsky, S. A., and Dowdy, S. F. (1998) *Nat. Med.* **4**, 1449–1452
45. Zhang, H., Ozaki, I., Mizuta, T., Yoshimura, T., Matsushashi, S., Hisatomi, A., Tadano, J., Sakai, T., and Yamamoto, K. (2003) *Hepatology* **38**, 305–313
46. Bachmann, M., and Möröy, T. (2005) *Int. J. Biochem. Cell Biol.* **37**, 726–730
47. Peters, J. M. (2006) *Nat. Rev. Mol. Cell Biol.* **7**, 644–656
48. Jaspersen, S. L., Charles, J. F., and Morgan, D. O. (1999) *Curr. Biol.* **9**, 227–236
49. Visintin, R., Craig, K., Hwang, E. S., Prinz, S., Tyers, M., and Amon, A. (1998) *Mol. Cell* **2**, 709–718
50. Zachariae, W., Schwab, M., Nasmyth, K., and Seufert, W. (1998) *Science* **282**, 1721–1724
51. Kramer, E. R., Scheuringer, N., Podtelejnikov, A. V., Mann, M., and Peters, J. M. (2000) *Mol. Biol. Cell* **11**, 1555–1569
52. van Leuken, R., Clijsters, L., and Wolthuis, R. (2008) *Biochim. Biophys. Acta* **1786**, 49–59
53. Sutterlüty, H., Chatelain, E., Marti, A., Wirbelauer, C., Senften, M., Müller, U., and Krek, W. (1999) *Nat. Cell Biol.* **1**, 207–214
54. Pogacic, V., Bullock, A. N., Fedorov, O., Filippakopoulos, P., Gasser, C., Biondi, A., Meyer-Monard, S., Knapp, S., and Schwaller, J. (2007) *Cancer Res.* **67**, 6916–6924
55. Choudhary, C., Olsen, J. V., Brandts, C., Cox, J., Reddy, P. N., Böhmer, F. D., Gerke, V., Schmidt-Arras, D. E., Berdel, W. E., Müller-Tidow, C., Mann, M., and Serve, H. (2009) *Mol. Cell* **36**, 326–339
56. Amaravadi, R., and Thompson, C. B. (2005) *J. Clin. Invest.* **115**, 2618–2624
57. Kraft, C., Vodermaier, H. C., Maurer-Stroh, S., Eisenhaber, F., and Peters, J. M. (2005) *Mol. Cell* **18**, 543–553
58. Hall, M. C., Warren, E. N., and Borchers, C. H. (2004) *Cell Cycle* **3**, 1278–1284
59. Bhattacharya, N., Wang, Z., Davitt, C., McKenzie, I. F., Xing, P. X., and Magnuson, N. S. (2002) *Chromosoma* **111**, 80–95
60. Roh, M., Gary, B., Song, C., Said-Al-Naief, N., Tousson, A., Kraft, A., Eltoun, I. E., and Abdulkadir, S. A. (2003) *Cancer Res.* **63**, 8079–8084
61. Roh, M., Song, C., Kim, J., and Abdulkadir, S. A. (2005) *J. Biol. Chem.* **280**, 40568–40577

The Pim protein kinases regulate energy metabolism and cell growth

Zanna Beharry^a, Sandeep Mahajan^b, Marina Zemskova^c, Ying-Wei Lin^d, Baby G. Tholanikunnel^b, Zuping Xia^a, Charles D. Smith^{a,b}, and Andrew S. Kraft^{b,1}

^aDepartment of Pharmaceutical and Biomedical Sciences, South Carolina College of Pharmacy, ^bHollings Cancer Center, ^cDepartment of Cell and Molecular Pharmacology, and ^dDepartment of Pediatrics, Medical University of South Carolina, Charleston, SC 29425

Edited by Peter K. Vogt, The Scripps Research Institute, La Jolla, CA, and approved November 19, 2010 (received for review September 3, 2010)

The serine/threonine Pim kinases are overexpressed in solid cancers and hematologic malignancies and promote cell growth and survival. Here, we find that a novel Pim kinase inhibitor, SMI-4a, or Pim-1 siRNA blocked the rapamycin-sensitive mammalian target of rapamycin (mTORC1) activity by stimulating the phosphorylation and thus activating the mTORC1 negative regulator AMP-dependent protein kinase (AMPK). Mouse embryonic fibroblasts (MEFs) deficient for all three Pim kinases [triple knockout (TKO) MEFs] demonstrated activated AMPK driven by elevated ratios of AMP:ATP relative to wild-type MEFs. Consistent with these findings, TKO MEFs were found to grow slowly in culture and have decreased rates of protein synthesis secondary to a diminished amount of 5'-cap-dependent translation. Pim-3 expression alone in TKO MEFs was sufficient to reverse AMPK activation, increase protein synthesis, and drive MEF growth similar to wild type. Pim-3 expression was found to markedly increase the protein levels of both c-Myc and the peroxisome proliferator-activated receptor gamma coactivator 1 α (PGC-1 α), enzymes capable of regulating glycolysis and mitochondrial biogenesis, which were diminished in TKO MEFs. Overexpression of PGC-1 α in TKO MEFs elevated ATP levels and inhibited the activation of AMPK. These results demonstrate the Pim kinase-mediated control of energy metabolism and thus regulation of AMPK activity. We identify an important role for Pim-3 in modulating c-Myc and PGC-1 α protein levels and cell growth.

LKB1 | mitochondria | mTOR | 4EBP1

The Pim serine/threonine kinases include three isoforms, Pim-1, Pim-2, and Pim-3, that are implicated in the growth and progression of hematological malignancies, prostate cancer, and, in the case of Pim-3, in precancerous and cancerous lesions of the pancreas, liver, colon, and stomach (1–5). Pim-1 and Pim-2 have been shown to cooperate with c-Myc in inducing lymphoma (6), and prostate cancer (7), and in the absence of Pim-1 and Pim-2, Pim-3 is activated in c-Myc-induced lymphomas (8). The mechanisms suggested to explain this Pim–Myc synergism include Pim-mediated stabilization of c-Myc protein (9) and regulation of gene transcription via Pim-1 phosphorylation of histone H3 at active sites of c-Myc transcription (10). Other Pim kinase substrates that suggest these enzymes play a role in cell cycle progression and antiapoptosis include BAD, Bcl-2, Bcl-xL (11, 12), p27^{Kip1} (13), and Cdc25A (14).

Recently, Pim kinases have been suggested to promote the activity of the rapamycin-sensitive mammalian target of rapamycin (mTORC1) (15–17). mTORC1 is a serine/threonine kinase that regulates cell growth and metabolism (18). The mTORC1 complex, composed of mTOR, raptor, G β L, and PRAS40, promotes protein synthesis by phosphorylating 4EBP1, thus stimulating its dissociation from the translational regulator eukaryotic initiation factor 4E (eIF4E) (17) allowing for cap-dependent translation. mTORC1 activity is regulated by a cascade of enzymes including LKB1, AMP-dependent protein kinase (AMPK), and TSC1 and 2 (19). AMPK senses the cellular energy status and is activated via LKB1-mediated phosphorylation when there is a decline in ATP

levels and concomitant rise in AMP levels; i.e., high AMP:ATP ratio (20). Activated AMPK down-regulates the energetically demanding process of protein synthesis by inhibiting mTORC1 activity through phosphorylating TSC2 and raptor (20). The mechanisms by which Pim kinase stimulates mTORC1 appear complex and include 4EBP1, eIF4E (16, 21–23), and PRAS40 phosphorylation (15).

Because of the importance of the Pim kinase signal transduction pathway in the progression of various cancers, multiple groups have developed small-molecule inhibitors of this kinase family (24–28). We have identified unique benzylidene-thiazolidine-2,4-diones (23, 29) that inhibit Pim kinase activity in vitro at nanomolar concentrations, and in culture induce apoptosis of human leukemic cells (30) and synergize with rapamycin to downregulate 4EBP1 phosphorylation and inhibit cell growth (29). Taking advantage of these inhibitors, siRNA, and genetically engineered Pim-deficient cells, we have discovered a unique role for Pim-3 in regulating mTORC1 activity through modulation of ATP levels by the induction of c-Myc and the transcriptional coactivator and master regulator of mitochondrial biogenesis peroxisome proliferator-activated receptor gamma coactivator 1 α (PGC-1 α).

Results

Pim Kinase Negatively Regulates AMPK. To examine the mechanisms by which Pim kinase can regulate the mTORC1 pathway, the human erythroleukemia cell line K562 was incubated with the thiazolidinedione Pim kinase inhibitor SMI-4a (23), and the phosphorylation of AMPK was studied. AMPK activation results in the phosphorylation of raptor and TSC2 and thus inhibits mTORC1 activity (20, 31). Pim kinase inhibition with SMI-4a induced the activation of AMPK as determined by phosphorylation of AMPK α at Thr172, and the AMPK targets acetyl-CoA carboxylase (ACC) at Ser79 and raptor at Ser792 and inhibition of mTORC1 activity as determined by decreased phosphorylation of the mTORC1 targets S6K and 4EBP1 (Fig. 1 *A* and *B*). Additionally, knockdown of Pim-1 levels with a targeted siRNA increased AMPK phosphorylation (Fig. 1*C*), suggesting that Pim-1 negatively regulates the phosphorylation of this enzyme. Because the LKB1 kinase is known to activate AMPK via phosphorylation at Thr172 (32) and loss of LKB1 activity is frequently associated with the transformed phenotype (32), we examined the ability of SMI-4a and SMI-16a, another Pim kinase inhibitor, (29) to regulate AMPK phosphorylation in a panel of LKB1-containing (H358, H661) and deficient (H23, H460, A549) lung cancer cell

Author contributions: Z.B. and A.S.K. designed research; Z.B., S.M., M.Z., Y.-W.L., and B.G.T. performed research; Z.B., S.M., M.Z., Y.-W.L., B.G.T., Z.X., and C.D.S. contributed new reagents/analytic tools; Z.B., S.M., M.Z., B.G.T., and A.S.K. analyzed data; and Z.B. and A.S.K. wrote the paper.

The authors declare no conflict of interest.

This article is a PNAS Direct Submission.

¹To whom correspondence should be addressed. E-mail: kraft@muscc.edu.

This article contains supporting information online at www.pnas.org/lookup/suppl/doi:10.1073/pnas.1013214108/-DCSupplemental.

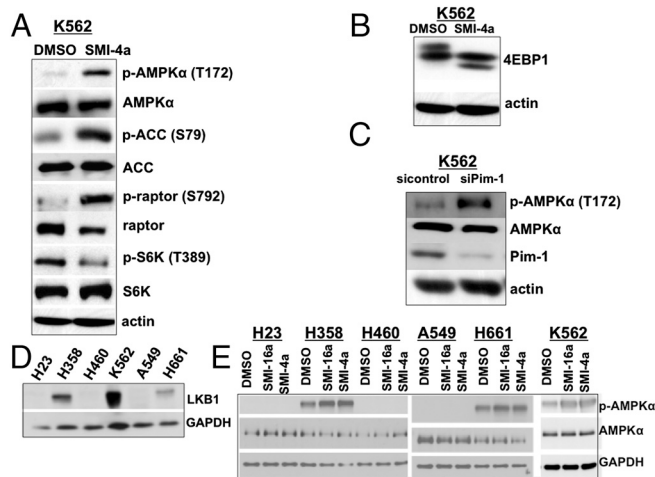


Fig. 1. Pim kinase inhibition activates AMPK. (A and B) K562 cells were treated with DMSO or SMI-4a (5 μ M) for 1 h in the absence of serum, and lysates were probed for the indicated proteins by Western blotting. (C) K562 cells were transfected with scrambled siRNA (siControl) or Pim-1 siRNA (siPim-1), and 48 h later lysates were probed for the indicated proteins by Western blotting. (D) Western blot for LKB1 levels in lung cancer cell lines and the leukemia cell line K562. (E) Lung and leukemia cells were treated with DMSO, SMI-4a, or SMI-16a (5 μ M) for 1 h in the absence of serum, and lysates were probed for the indicated proteins by Western blotting.

lines along with the LKB1-positive K562 cell line (Fig. 1D). These results demonstrate that the Pim kinase inhibitors SMI-4a and SMI-16a required LKB1 to stimulate AMPK activity (Fig. 1E).

To further confirm that Pim kinase regulates the activation of AMPK, we generated mouse embryonic fibroblasts (MEFs) deficient for Pim-1, -2, and -3 [triple knockout (TKO)] (33),

and wild-type (WT) littermate control MEFs. Consistent with both the siRNA and small-molecule inhibition of Pim kinase activity, TKO MEFs had significantly higher AMPK phosphorylation compared to WT MEFs (Fig. 2A). To determine the contribution of each Pim isoform to AMPK activation, TKO MEFs were transduced with Pim-1, -2, or -3 lentiviruses. Although each Pim isoform reduced p-AMPK levels, Pim-3 showed the greatest effect (Fig. S1A) leading us to focus on elucidating the unique role of Pim-3. To confirm this result, we generated MEFs deficient in Pim-1 and Pim-2 (Pim-1^{-/-}, -2^{-/-}, -3^{+/+}) but expressing Pim-3, and demonstrated that these cells showed less activated AMPK than TKO MEFs (Fig. 2A). As AMPK activation is regulated by increased AMP, we measured the levels of AMP and ATP and found that AMPK phosphorylation correlates with the cellular AMP:ATP ratio in these knockout MEFs (Fig. 2B). Growth curves of these MEFs demonstrated a further correlation between proliferation, AMP:ATP ratio, and AMPK phosphorylation status (Fig. 2C) with the TKO MEFs showing the slowest growth rate. Similar results were obtained with immortalized WT or TKO MEFs transduced with empty vector or a lentivirus expressing Pim-3 (Fig. S1B).

Because activation of AMPK leads to inhibition of mTORC1 activity (31), we measured the level of protein synthesis in each of the MEFs. Labeling of MEFs with ³⁵S-methionine and measuring newly synthesized protein demonstrated, as predicted, that TKO MEFs when compared to WT have lower rates of protein synthesis (approximately 58% relative to WT). Expression of Pim-3 in the TKO cells increased protein synthesis from 58% (TKO) to 83% relative to WT (Fig. 2D). Consistent with this result, we found that in TKO MEFs the cap-dependent but not internal ribosome entry site (IRES)-dependent translational activity is reduced (Fig. 2E). Cap-dependent translation depends on the mTORC1-mediated release of 4EBP1 from eIF4E and the for-

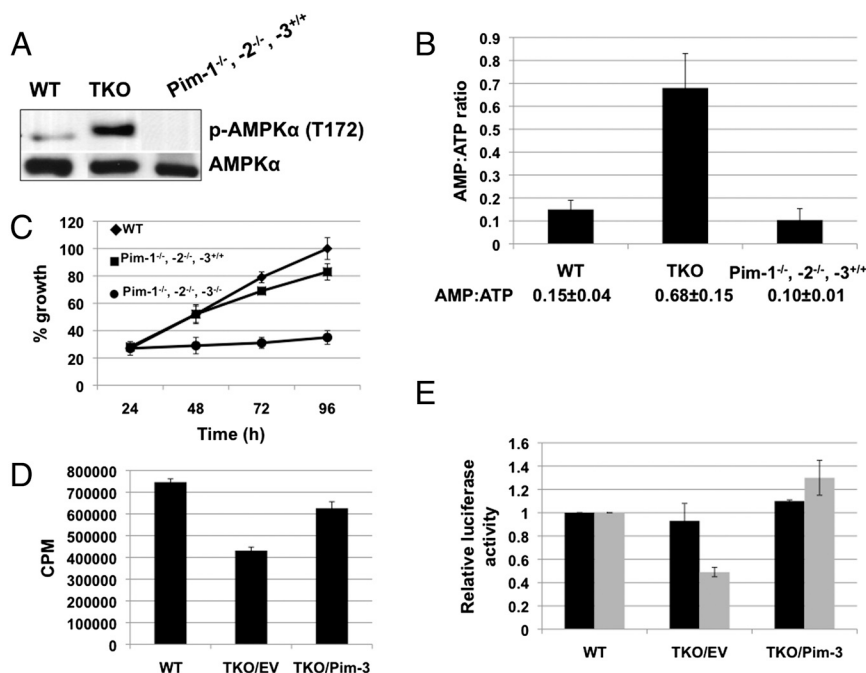


Fig. 2. Knockout of Pim kinase isoforms inhibits protein synthesis and cell growth. (A) Lysates were prepared from the different MEF cell lines and probed for the indicated proteins by Western blotting. (B) AMP:ATP ratios were determined by HPLC as described in *Materials and Methods*. Values are the average of three independent experiments, and the standard deviation from the mean is shown. (C) Growth curve of MEFs as determined by MTT assay. Percentage values are relative to the growth of WT MEFs at the 96 h time point (100%). The data points are the average of three independent measurements, and the standard deviation from the mean is shown. (D) ³⁵S-methionine incorporation into WT and TKO MEFs expressing empty vector (TKO/EV) or Pim-3 (TKO/Pim-3). Values (cpm/mg protein) are the average of three independent measurements, and the standard deviation from the mean is shown. (E) Cap-dependent (gray bars) and IRES-dependent (black bars) translation in MEFs as measured by Renilla and Firefly luciferase activities, respectively. As described in *Materials and Methods*, MEFs were infected with a virus expressing cap- and IRES-driven luciferase constructs. Values are the ratio of luciferase activity relative to WT and are the average of three independent measurements with the standard deviation from the mean shown.

mation of the eIF4F complex. Using m⁷-GTP beads in a pull-down assay (34), we found that in TKO MEFs eIF4E is highly bound to 4EBP1, whereas eIF4G binding is lost and thus the ability of eIF4E to promote translation is inhibited (Fig. S1C). These results demonstrate that reduced Pim kinase activity correlates with increased AMP:ATP ratio, activation of AMPK, inhibition of mTORC1 activity, and reduced overall protein synthesis.

Pim-3 Regulates c-Myc Levels. In comparison to TKO MEFs, Pim-3-expressing cells demonstrated increased 5'-cap-dependent protein synthesis and growth similar to WT MEFs. Because the levels of the c-Myc protein are controlled by 5'-cap-dependent transcription, and c-Myc is important in the regulation of both cell growth and overall cellular metabolism, we examined the levels of c-Myc in MEFs from each genotype. Western blots demonstrate that the expression of Pim-3 either in primary MEFs (Fig. 3A) or after transduction into TKO MEFs (Fig. 3B) markedly increased c-Myc protein. Similar to p-AMPK (Fig. S14), neither Pim-1 nor Pim-2 was able to induce the significant levels of c-Myc protein observed with Pim-3 overexpression in TKO MEFs (Fig. 3B). Furthermore, expression of Pim-1 or Pim-2 in Pim-3-only MEFs led to a decrease in c-Myc protein levels (Fig. S1D), suggesting the possibility that the Pim kinases could compete for substrates or interact directly. Because of the marked difference in c-Myc protein levels in MEFs containing Pim-3 only, we tested two additional MEF cell lines generated from different embryos of the same genotype and again observed increased c-Myc protein levels (Fig. S2B). To determine whether the increased c-Myc level in Pim-3-expressing cells is unique to MEFs in culture, we measured the c-Myc levels in spleen lysates of 4-mo-old WT, TKO, and Pim-1^{-/-}, -2^{-/-}, -3^{+/+} mice and again found the highest level of c-Myc protein in the Pim-3-only genotype (Fig. S2C). Because deletion of one Pim might grossly elevate the level of another, in this case Pim-3, we measured the level of Pim-3 mRNA in the different MEF genotypes but did not find a significant difference (Fig. S24). These results suggested that Pim-3 might modulate c-Myc translation.

To determine the effect of Pim-3 on c-Myc translation, we treated MEFs with cycloheximide until c-Myc protein was completely degraded, washed out the cycloheximide, and then monitored by Western blotting the rate of increase in c-Myc protein over time. To make this comparison possible, 2.5 times more protein from TKO MEFs was loaded on these SDS gels. TKO MEFs showed a delay in protein synthesis with only 53 and 43% as much c-Myc protein synthesis in the first 15 min when compared to WT and TKO/Pim-3 MEFs, respectively (Fig. 3C). This result is consistent with the reduced protein synthesis in the TKO MEFs (Fig. 2D). Because the overall translational efficiency in cells is reflected by changes in the polysome/monosome ratio, we determined the polysome profile using cytosolic extracts of WT, TKO, and TKO/Pim-3 cells. TKO cells showed a significant reduction in heavy polysomes and a corresponding increase in free ribosome subunits (Fig. 3D Upper). However, expression of Pim-3 in TKO cells resulted in a significant increase in heavy polysomes. c-Myc mRNA showed redistribution from heavy toward lighter polysomes and monosomes and free subunits in TKO cells relative to WT (Fig. 3D Lower). This shift was reversed by Pim-3 expression, suggesting that Pim-3 is capable of controlling the translation of c-Myc mRNA (Fig. 3D Lower). Because Pim-1 and -2 have been shown to increase the stability of c-Myc (9), we examined changes in c-Myc protein stability in TKO and TKO/Pim-3 MEFs after cycloheximide treatment but found no significant difference in c-Myc half-life in the Pim-3-containing cells (Fig. S2D). Finally, we found that the expression of c-Myc in TKO MEFs led to a decrease in AMPK activation (Fig. S2E) consistent with the ability of c-Myc to stimulate cell growth.

Pim-3 and c-Myc Regulate PGC-1 α Levels. The differences in the growth rate between the TKO and Pim-3 only MEFs could possibly be explained by the Pim-3-mediated increased c-Myc because the latter is known to control multiple factors that regulate cell growth and metabolism (35, 36). Therefore, we compared the growth rate of TKO MEFs stably expressing empty vector, Pim-3, or c-Myc to WT MEFs. The TKO/c-Myc MEFs were able to

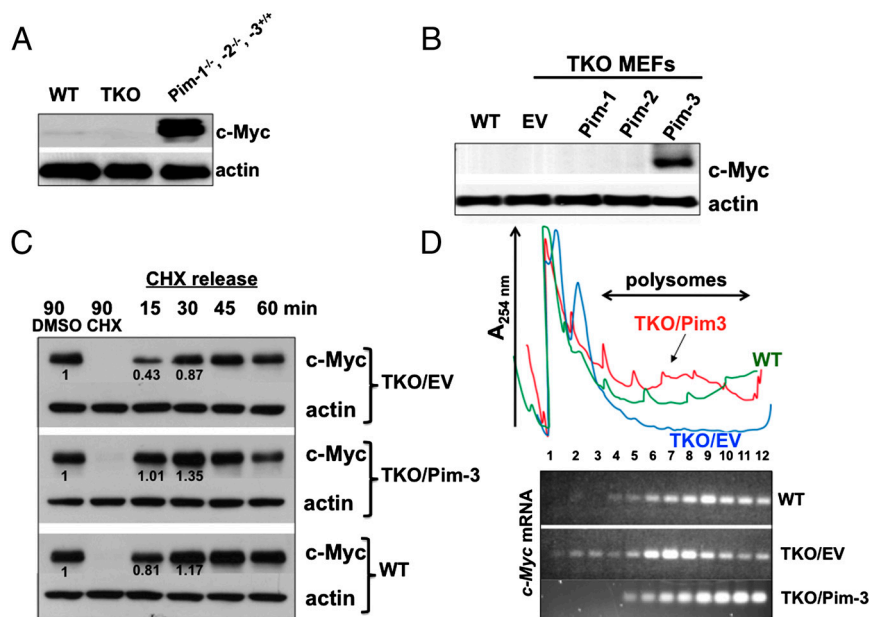


Fig. 3. Pim-3 elevates c-Myc levels. (A) c-Myc protein levels in each MEF genotype as determined by Western blotting. (B) TKO MEFs were infected with empty vector (EV), Pim-1, -2, or -3 lentiviruses, and 48 h later lysates were probed for c-Myc levels and compared to WT MEFs. (C) TKO MEFs expressing EV or Pim-3 were treated for 90 min with cycloheximide (CHX, 10 μ M), the media replaced, and lysates probed for c-Myc levels by Western blotting. Densitometry analysis was performed, and the values at the 15 min time point relative to DMSO are shown. To obtain a relatively equal amount of c-Myc protein at the 90 min time point with DMSO, ~2.5-fold more TKO/EV protein lysate was loaded relative to TKO/Pim-3. (D) Ribosome fractions of WT and TKO MEFs expressing EV or Pim-3 were prepared by sucrose gradient (see *Materials and Methods*), and the level of c-Myc mRNA associated with each fraction was determined by PCR.

grow in the absence of Pim kinases but did not reach the same density in 96 h (Fig. 4A). The shRNA-mediated knockdown of c-Myc in TKO/Pim-3 MEFs did not completely inhibit cell proliferation (Fig. 4B). Together, these results suggest that Pim-3 and c-Myc do not have completely overlapping biologic activities. To understand how Pim-3 decreases the AMP:ATP ratio and inhibits AMPK phosphorylation, we measured the levels of PGC-1 α . PGC-1 α activates a wide variety of transcription factors that result in increased mitochondrial biogenesis and oxidative phosphorylation (37). Increased expression of PGC-1 α can lead to elevations in ATP levels (38), whereas PGC-1 α knockout leads to reduced ATP levels in murine hearts (39). PGC-1 α expression and PGC-1 α -dependent gene expression are induced by chemical activation of AMPK, and AMPK directly phosphorylates PGC-1 α , leading to increased transcriptional activity (40–42). We found that the levels of PGC-1 α mRNA and protein were greatly reduced in TKO MEFs, highest in Pim-3-only MEFs, and intermediate in WT cells (Fig. 4C and D). To examine the contributions of Pim-3 and c-Myc in regulating PGC-1 α levels, we infected TKO MEFs with lentiviruses expressing c-Myc or Pim-3 and found that Pim-3 induced marked increases in PGC-1 α mRNA (12-fold) and protein; the effect of c-Myc alone was a 4-fold increase in mRNA, and the increase in protein was quantitated at only 10% that of Pim-3 (Fig. 4D, E).

The above results suggest that the increased AMP:ATP ratio in TKO MEFs may be attributed to low ATP levels due to decreased PGC-1 α protein, thus leading to AMPK activation. To examine whether overexpression of PGC-1 α in TKO MEFs was sufficient to reduce p-AMPK by increasing the level of cellular ATP, we transduced TKO MEFs with a lentivirus expressing PGC-1 α . Western blots and biochemical analysis demonstrate that PGC-1 α expression in TKO MEFs decreased the level of p-AMPK (Fig. 5A) and increased the levels of ATP (Fig. 5B), leading to decreased 4EBP1 binding to eIF4E while increasing

eIF4G association with the eIF4E protein (Fig. S3). In contrast, PGC-1 α expression in TKO MEFs showed little effect on c-Myc levels (Fig. 5A). Thus, Pim-3, by controlling the levels of both c-Myc and PGC-1 α , is able to impact on AMPK phosphorylation, mTORC1 activity, 5'-cap-dependent translation, and ultimately cell growth (Fig. 5C).

Discussion

The combined approach of genetic knockout, RNAi, and small-molecule inhibition implicate the Pim kinases in regulating the AMP:ATP ratio and energy metabolism. These effects lead to the modulation of the mTORC1 pathway by AMPK and the control of cell growth. In leukemic cells, the pan-Pim kinase inhibitor SMI-4a stimulated the phosphorylation and activation of AMPK, whereas in TKO MEFs the ratio of AMP:ATP was markedly increased and AMPK was activated. Because AMPK is a negative regulator of mTORC1, we found in leukemic cells treated with SMI-4a and in TKO MEFs that mTORC1 activity is inhibited and cap-dependent translation is significantly decreased. In MEFs, the expression of Pim-3 alone could reverse these processes, lowering the AMP:ATP ratio, decreasing the activation of AMPK, and increasing cap-dependent translation, all resulting in cellular growth rates comparable to WT MEFs. The differences between the TKO and Pim-3-only MEFs could be explained in part by the Pim-3-mediated increased c-Myc because the latter controls multiple transcription factors that regulate cell growth and metabolism (35, 36). Infection of TKO MEFs with a lentivirus expressing c-Myc increased the growth of these cells but did not duplicate the growth curve of Pim-3-expressing MEFs.

In muscle and fat tissue, the ability of activated AMPK to maintain an energy balance is achieved in part by stimulating PGC-1 α (41). The ability of PGC-1 α to coactivate multiple transcription factors makes this protein a master regulator of mitochondrial biogenesis (43). Considering this link between

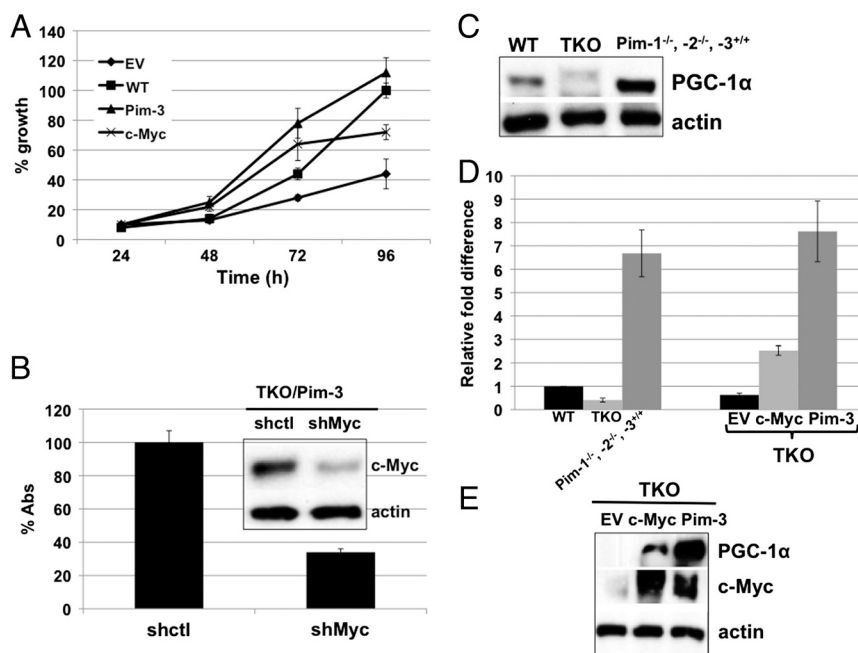


Fig. 4. Pim-3 and c-Myc affect PGC-1 α levels. (A) Growth curve of TKO MEFs expressing empty vector (EV), c-Myc, or Pim-3 as determined by an MTT assay. Percentage values are relative to the value of WT MEFs at the 96 h time point (100%). The data points are the average of three independent measurements, and the standard deviation from the mean is shown. (B) TKO/Pim-3 MEFs were infected with nontargeting shRNA (shctl) or c-Myc targeting shRNA (shMyc) lentiviruses. Equal numbers of shctl and shMyc cells were plated 48 h postinfection, and after an additional 72 h viability was determined by an MTT assay and represented as a percent absorbance (%Abs) with shctl set at 100%. The data points are the average of three independent measurements, and the standard deviation from the mean is shown. (Inset) Lysates were prepared at 120 h postinfection and probed for the indicated proteins by Western blotting. (C) PGC-1 α protein levels in MEFs as determined by Western blotting. (D) PGC-1 α mRNA levels in primary MEFs (WT, TKO, Pim-1^{-/-}, -2^{-/-}, -3^{+/+}) or TKO MEFs infected with EV, c-Myc, or Pim-3 lentiviruses as determined by QT-PCR 48 h after infection. Values are the average of three independent measurements, and the standard deviation from the mean is shown. (E) PGC-1 α protein levels as determined by Western blotting in TKO MEFs 48 h postinfection with EV, c-Myc, or Pim-3.

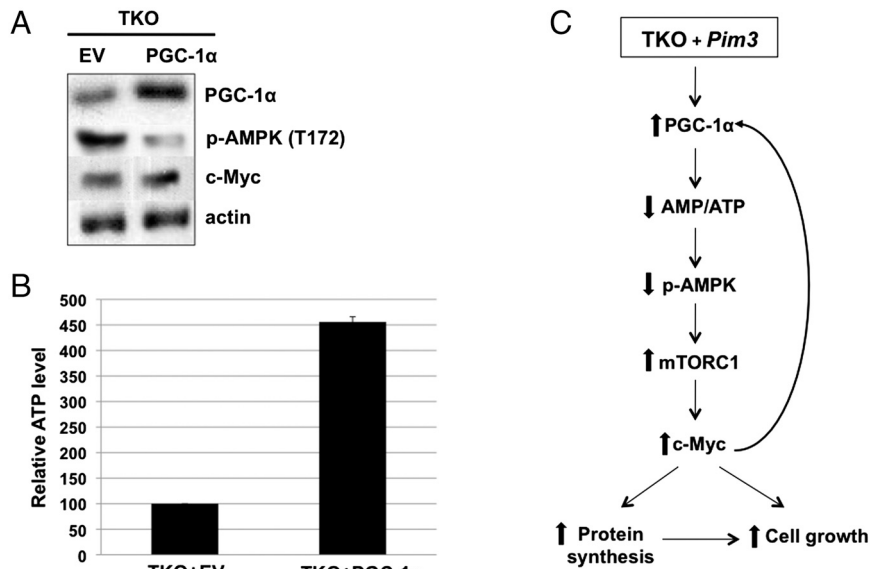


Fig. 5. Expression of PGC-1 α restores the AMP:ATP ratio in TKO MEFs. (A) PGC-1 α overexpression in TKO MEFs reduces AMPK activation. Lysates were prepared from TKO MEFs 48 h after transduction with empty vector (EV) or PGC-1 α lentiviruses, and protein levels compared by Western blotting. (B) ATP levels determined in lysates from Fig. 5A as described in *Materials and Methods*. Values are the average of three independent measurements, and the standard deviation from the mean is shown. (C) Schematic summary of biologic changes observed in TKO MEFs expressing Pim-3.

AMPK and PGC-1 α in the sensing and regulation of the cell's energy status, the levels of PGC-1 α were investigated and found to be significantly lower in TKO MEFs. In comparison, Pim-3-containing MEFs showed increased levels of PGC-1 α relative to WT. Therefore, in the case of the TKO MEFs, chronic AMPK activation coupled with drastically reduced levels of PGC-1 α protein resulted in an elevated AMP:ATP ratio. Accordingly, infection of TKO MEFs with a lentivirus expressing PGC-1 α was shown to increase ATP levels and decrease AMPK activation. The increased PGC-1 α levels in Pim-3-only MEFs cannot be attributed solely to increased c-Myc because TKO/c-Myc MEFs showed lower levels of PGC-1 α mRNA and protein relative to TKO/Pim-3 MEFs. This suggests the possibility that Pim-3 and c-Myc could cooperate in regulating PGC-1 α levels in MEFs. This cooperation may extend beyond transcription/translation because PGC-1 α levels and activity are regulated by multiple posttranslational mechanisms (37).

Pim-3 is the least-studied kinase of the Pim family; however, it has been linked to the development and progression of colon and pancreatic cancers (2–4, 44). Despite the high sequence identity and overlapping substrate specificity of the Pim kinases, Pim-3 expression alone is shown to overcome at least some of the defects found in the loss of both Pim-1 and Pim-2, including growth rate. Additionally, the knockout of Pim-1 and -2 and the expression of Pim-3 only led to a marked increase in c-Myc protein relative to WT MEFs. The observation that the transduction of Pim-1 or -2 into MEFs containing Pim-3 suppressed c-Myc levels suggested the possibility that individual Pim isoforms may regulate each other either directly or through substrate competition. This poses the question of whether Pim isoforms either individually or acting in concert regulate different biological processes and under what cellular circumstances. The question of the activity of Pim isoforms is of importance to the design of small-molecule inhibitors targeting these kinases and their use in the treatment of diseases, including cancer. Both Pim-1 and -2 are known to enhance c-Myc-induced transformation (6, 12) and phosphorylate and stabilize c-Myc protein, leading to increased transcriptional activity (9). In the MEFs used in this study, Pim-3 expression alone enhanced cap-dependent translation, increased c-Myc levels without changing the protein's stability, and increased the cell growth rate. Because elevated levels of both Pim-3 and c-Myc are found in

gastrointestinal cancers, our results suggest the possibility that Pim-3 might enhance the growth of these tumor cells in part by regulating c-Myc levels, thus highlighting the potential utility of Pim-3 targeted inhibitors.

Materials and Methods

Cell Culture. MEFs were derived from 14.5-d-old embryos and were genotyped as described (45). For stable cell lines, TKO MEFs were transduced with lentiviruses encoding empty vector, PIM-1, Pim-2, Pim-3, or c-Myc and selected with puromycin (4 μ g/mL).

Construction of Lentiviral Vectors. The open reading frames of PIM-1 (human, 33 kDa isoform), PIM-2 (mouse), Pim-3 (mouse), c-Myc (mouse), and PGC-1 α (human, a gift from Young-In Chi, Department of Molecular and Cellular Biochemistry, University of Kentucky, Lexington, KY) were amplified by PCR from full-length cDNA clones and subcloned into the *AgeI-MluI* sites of pLex-MCS lentiviral vector (Open Biosystems). Methods for preparation of lentiviral stocks are detailed in *SI Materials and Methods*.

Quantitative RT-PCR (QT-PCR). Total RNA was isolated from MEFs using the RNeasy kit (Qiagen) according to the manufacturer's protocol. The first-strand cDNA was synthesized using Superscript first-strand synthesis kit and Oligo (dT) primer (Invitrogen).

Biochemical Analysis. K562 cells were transfected with scrambled siRNA or siPim-1 (ON-TARGETplus SMARTpool, Thermo Scientific) using LipofectamineTM2000 (Invitrogen) according to the manufacturer's protocol, and 48 h posttransfection lysates were prepared. Cell growth was measured using the 3-(4,5-dimethylthiazol-2-yl)-2,5-diphenyl tetrazolium bromide (MTT) assay. ATP, ADP, and AMP were measured by HPLC as described previously (46), and ATP was also measured using the ATP Bioluminescence Assay Kit HS II (Roche) with 10^5 cells. eIF4E was captured on m⁷-GTP sepharose (GE Lifesciences) from WT and TKO MEFs lysate and bound 4EBP1 and eIF4G determined by Western blotting.

³⁵S-Methionine Incorporation. Cells were serum starved for 1 h in methionine-free medium (Invitrogen), followed by labeling with 100 mCi of ³⁵S-methionine/mL. Lysates and labeled proteins were precipitated with trichloroacetic acid on glass microfiber filters (Whatman) using vacuum filtration, and ³⁵S-incorporation was counted.

Cap- vs. IRES-Dependent Translation. A bicistronic retroviral vector, pMSCV/rLuc-pol IRES-fLuc (a gift from Peter B. Bitterman, Department of Medicine, University of Minnesota, Minneapolis, MN), was used to produce viral particles for infecting WT, TKO and TKO/Pim-3 MEFs. Cells were collected

48 hr postinfection and Renilla/Firefly luciferase activities were quantified using the dual-luciferase reporter assay system (Promega) and a luminometer according to the manufacturer's instructions.

Polysome Profile Analysis. Sucrose density gradient centrifugation was employed to separate the ribosome fractions as described previously (47). c-Myc mRNA level in each fraction was measured by PCR.

- Shah N, et al. (2008) Potential roles for the PIM1 kinase in human cancer—A molecular and therapeutic appraisal. *Eur J Cancer* 44:2144–2151.
- Fujii C, et al. (2005) Aberrant expression of serine/threonine kinase Pim-3 in hepatocellular carcinoma development and its role in the proliferation of human hepatoma cell lines. *Int J Cancer* 114:209–218.
- Li YY, et al. (2006) Pim-3, a proto-oncogene with serine/threonine kinase activity, is aberrantly expressed in human pancreatic cancer and phosphorylates bad to block bad-mediated apoptosis in human pancreatic cancer cell lines. *Cancer Res* 66:6741–6747.
- Popivanova BK, et al. (2007) Proto-oncogene, Pim-3 with serine/threonine kinase activity, is aberrantly expressed in human colon cancer cells and can prevent Bad-mediated apoptosis. *Cancer Sci* 98:321–328.
- White E (2003) The pims and outs of survival signaling: Role for the Pim-2 protein kinase in the suppression of apoptosis by cytokines. *Genes Dev* 17:1813–1816.
- Allen JD, Verhoeven E, Domen J, van der Valk M, Berns A (1997) Pim-2 transgene induces lymphoid tumors, exhibiting potent synergy with c-myc. *Oncogene* 15:1133–1141.
- Wang J, et al. (2010) Pim1 kinase synergizes with c-MYC to induce advanced prostate carcinoma. *Oncogene* 29:2477–2487.
- Mikkers H, et al. (2002) High-throughput retroviral tagging to identify components of specific signaling pathways in cancer. *Nat Genet* 32:153–159.
- Zhang Y, Wang Z, Li X, Magnuson NS (2008) Pim kinase-dependent inhibition of c-Myc degradation. *Oncogene* 27:4809–4819.
- Zippo A, De Robertis A, Serafini R, Oliviero S (2007) PIM1-dependent phosphorylation of histone H3 at serine 10 is required for MYC-dependent transcriptional activation and oncogenic transformation. *Nat Cell Biol* 9:932–944.
- Macdonald A, et al. (2006) Pim kinases phosphorylate multiple sites on Bad and promote 14-3-3 binding and dissociation from Bcl-XL. *BMC Cell Biol* 7:1.
- Shirogane T, et al. (1999) Synergistic roles for Pim-1 and c-Myc in STAT3-mediated cell cycle progression and antiapoptosis. *Immunity* 11:709–719.
- Morishita D, Katayama R, Sekimizu K, Tsuruo T, Fujita N (2008) Pim kinases promote cell cycle progression by phosphorylating and down-regulating p27Kip1 at the transcriptional and posttranscriptional levels. *Cancer Res* 68:5076–5085.
- Bachmann M, et al. (2006) The oncogenic serine/threonine kinase Pim-1 directly phosphorylates and activates the G2/M specific phosphatase Cdc25C. *Int J Biochem Cell Biol* 38:430–443.
- Zhang F, et al. (2009) PIM1 protein kinase regulates PRAS40 phosphorylation and mTOR activity in FDCP1 cells. *Cancer Biol Ther* 8:846–853.
- Hammerman PS, Fox CJ, Birnbaum MJ, Thompson CB (2005) Pim and Akt oncogenes are independent regulators of hematopoietic cell growth and survival. *Blood* 105:4477–4483.
- Laplante M, Sabatini DM (2009) mTOR signaling at a glance. *J Cell Sci* 122:3589–3594.
- Gibbons JJ, Abraham RT, Yu K (2009) Mammalian target of rapamycin: Discovery of rapamycin reveals a signaling pathway important for normal and cancer cell growth. *Semin Oncol* 36:53–517.
- Bai X, Jiang Y (2010) Key factors in mTOR regulation. *Cell Mol Life Sci* 67:239–253.
- Shaw RJ (2009) LKB1 and AMP-activated protein kinase control of mTOR signalling and growth. *Acta Physiol* 196:65–80.
- Chen WW, Chan DC, Donald C, Lilly MB, Kraft AS (2005) Pim family kinases enhance tumor growth of prostate cancer cells. *Mol Cancer Res* 3:443–451.
- Lilly M, Kraft A (1997) Enforced expression of the Mr 33,000 Pim-1 kinase enhances factor-independent survival and inhibits apoptosis in murine myeloid cells. *Cancer Res* 57:5348–5355.
- Xia Z, et al. (2009) Synthesis and evaluation of novel inhibitors of Pim-1 and Pim-2 protein kinases. *J Med Chem* 52:74–86.
- Pogacic V, et al. (2007) Structural analysis identifies imidazo[1,2-b]pyridazines as PIM kinase inhibitors with in vitro antileukemic activity. *Cancer Res* 67:6916–6924.
- Akue-Gedu R, et al. (2009) Synthesis, kinase inhibitory potencies, and in vitro antiproliferative evaluation of new Pim kinase inhibitors. *J Med Chem* 52:6369–6381.
- Chen LS, Redkar S, Bearss D, Wierda WG, Gandhi V (2009) Pim kinase inhibitor, SGI-1776, induces apoptosis in CLL lymphocytes. *Blood* 114:4150–4157.
- Grey R, et al. (2009) Structure-based design of 3-aryl-6-amino-triazolo[4,3-b]pyridazine inhibitors of Pim-1 kinase. *Bioorg Med Chem Lett* 19:3019–3022.
- Tong Y, et al. (2008) Isoxazolo[3,4-b]quinoline-3,4-(1H,9H)-diones as unique, potent and selective inhibitors for Pim-1 and Pim-2 kinases: Chemistry, biological activities, and molecular modeling. *Bioorg Med Chem Lett* 18:5206–5208.
- Beharry Z, et al. (2009) Novel benzylidene-thiazolidine-2,4-diones inhibit Pim protein kinase activity and induce cell cycle arrest in leukemia and prostate cancer cells. *Mol Cancer Ther* 8:1473–1483.
- Lin Y, et al. (2009) A small molecule inhibitor of Pim protein kinases blocks the growth of precursor T-cell lymphoblastic leukemia/lymphoma. *Blood* 115:824–833.
- Gwinn DM, et al. (2008) AMPK phosphorylation of raptor mediates a metabolic checkpoint. *Mol Cell* 30:214–226.
- Hezel AF, Bardeesy N (2008) LKB1; linking cell structure and tumor suppression. *Oncogene* 27:6908–6919.
- Mikkers H, et al. (2004) Mice deficient for all PIM kinases display reduced body size and impaired responses to hematopoietic growth factors. *Mol Cell Biol* 24:6104–6115.
- Connolly E, Braunstein S, Formenti S, Schneider RJ (2006) Hypoxia inhibits protein synthesis through a 4E-BP1 and elongation factor 2 kinase pathway controlled by mTOR and uncoupled in breast cancer cells. *Mol Cell Biol* 26:3955–3965.
- Liu YC, et al. (2008) Global regulation of nucleotide biosynthetic genes by c-Myc. *PLoS One* 3:e2722.
- Li F, et al. (2005) Myc stimulates nuclear encoded mitochondrial genes and mitochondrial biogenesis. *Mol Cell Biol* 25:6225–6234.
- Canto C, Auwerx J (2009) PGC-1alpha, SIRT1 and AMPK, an energy sensing network that controls energy expenditure. *Curr Opin Lipidol* 20:98–105.
- Liang H, Bai Y, Li Y, Richardson A, Ward WF (2007) PGC-1alpha-induced mitochondrial alterations in 3T3 fibroblast cells. *Ann NY Acad Sci* 1100:264–279.
- Arany Z, et al. (2005) Transcriptional coactivator PGC-1 alpha controls the energy state and contractile function of cardiac muscle. *Cell Metab* 1:259–271.
- Suwa M, Nakano H, Kumagai S (2003) Effects of chronic AICAR treatment on fiber composition, enzyme activity, UCP3, and PGC-1 in rat muscles. *J Appl Physiol* 95:960–968.
- Jäger S, Handschin C, St.-Pierre J, Spiegelman BM (2007) AMP-activated protein kinase (AMPK) action in skeletal muscle via direct phosphorylation of PGC-1α. *Proc Natl Acad Sci USA* 104:12017–12022.
- Irrcher I, Ljubcic V, Kirwan AF, Hood DA (2008) AMP-activated protein kinase-regulated activation of the PGC-1alpha promoter in skeletal muscle cells. *PLoS One* 3:e3614.
- Finley LW, Haigis MC (2009) The coordination of nuclear and mitochondrial communication during aging and calorie restriction. *Ageing Res Rev* 8:173–188.
- Li YY, Wu Y, Tsuneyama K, Baba T, Mukaida N (2009) Essential contribution of Ets-1 to constitutive Pim-3 expression in human pancreatic cancer cells. *Cancer Sci* 100:396–404.
- Xu J (2005) Preparation, culture, and immortalization of mouse embryonic fibroblasts. *Curr Protoc Mol Biol* Chap 28: Unit 28.1.
- Hahn-Windgassen A, et al. (2005) Akt activates the mammalian target of rapamycin by regulating cellular ATP level and AMPK activity. *J Biol Chem* 280:32081–32089.
- Ishimaru D, et al. (2009) Regulation of Bcl-2 expression by HuR in HL60 leukemia cells and A431 carcinoma cells. *Mol Cancer Res* 7:1354–1366.

SUPPORTING DATA

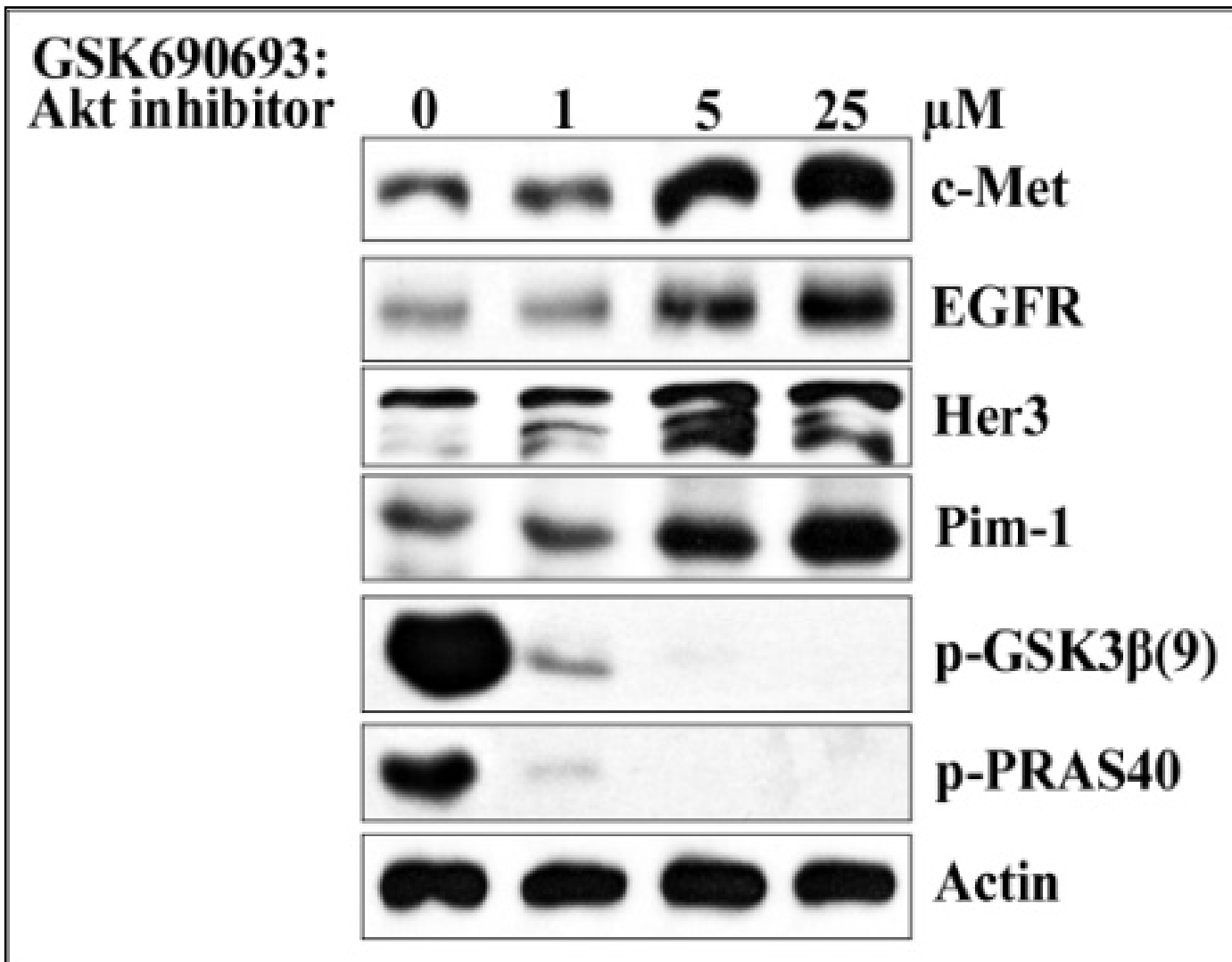


Figure 1: AKT inhibition induces increases in receptor tyrosine kinases and the Pim-1 protein kinase. PC3-LN4 cells were treated with varying amounts of AKT inhibitor for 24h, and western blots of extracts were done.

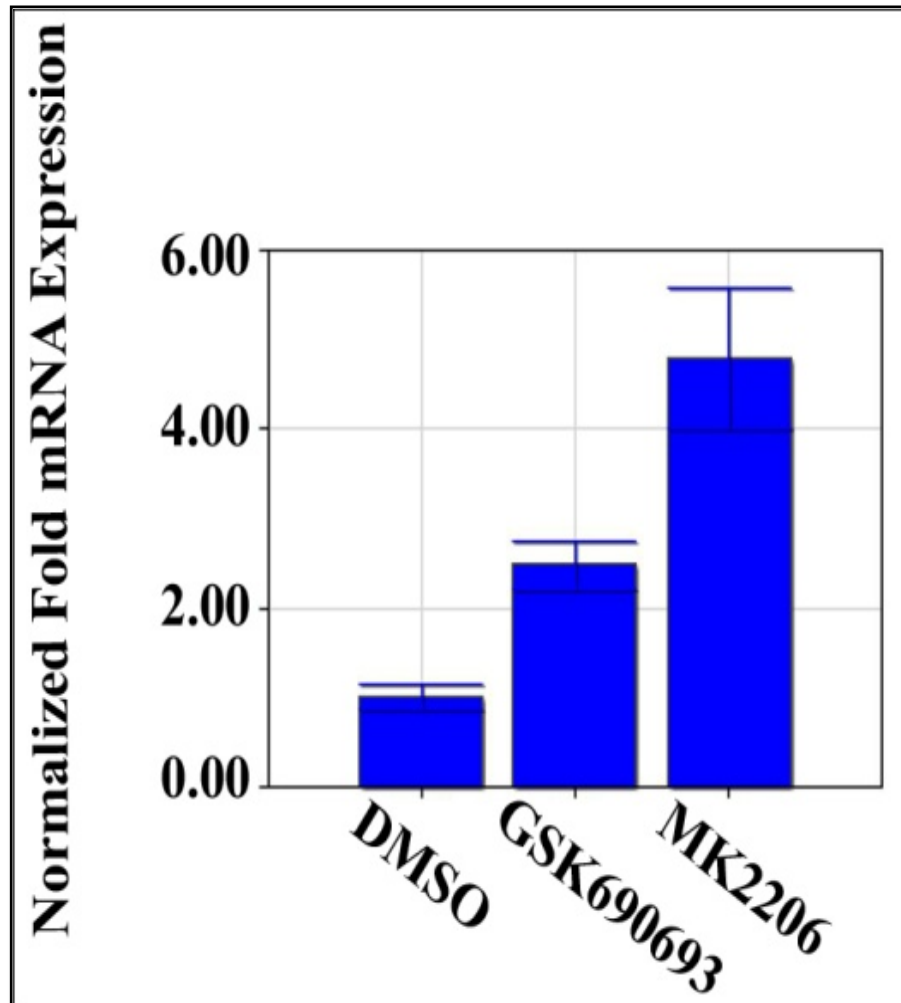


Figure 2: PIM-1 mRNA levels are stimulated by AKT inhibitors. PC3-LN4 were treated with GSK690693 or MK2206 (10 μ M) for 18h and mRNA isolated. qRT-PCR was done using β -actin as a control. The S.D. of triplicate experiments is shown.

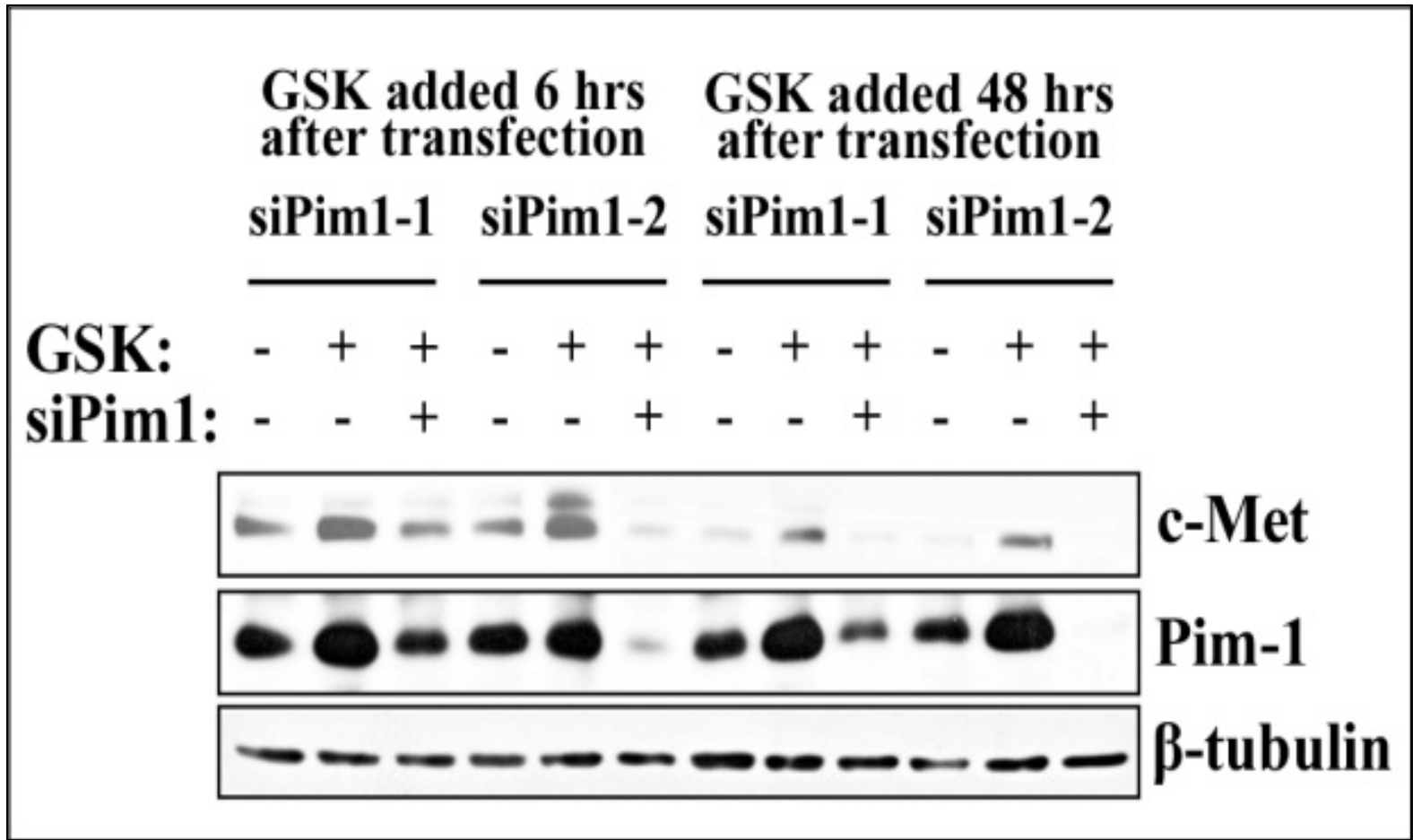


Figure 3a: Pim-1 is required for AKT inhibitor-induced c-Met up-regulation. PC3-LN4 cells were transfected with two different Pim-1 siRNAs and 24h later GSK690693 was added (10µM) for 6 or 48h and western blots were done.

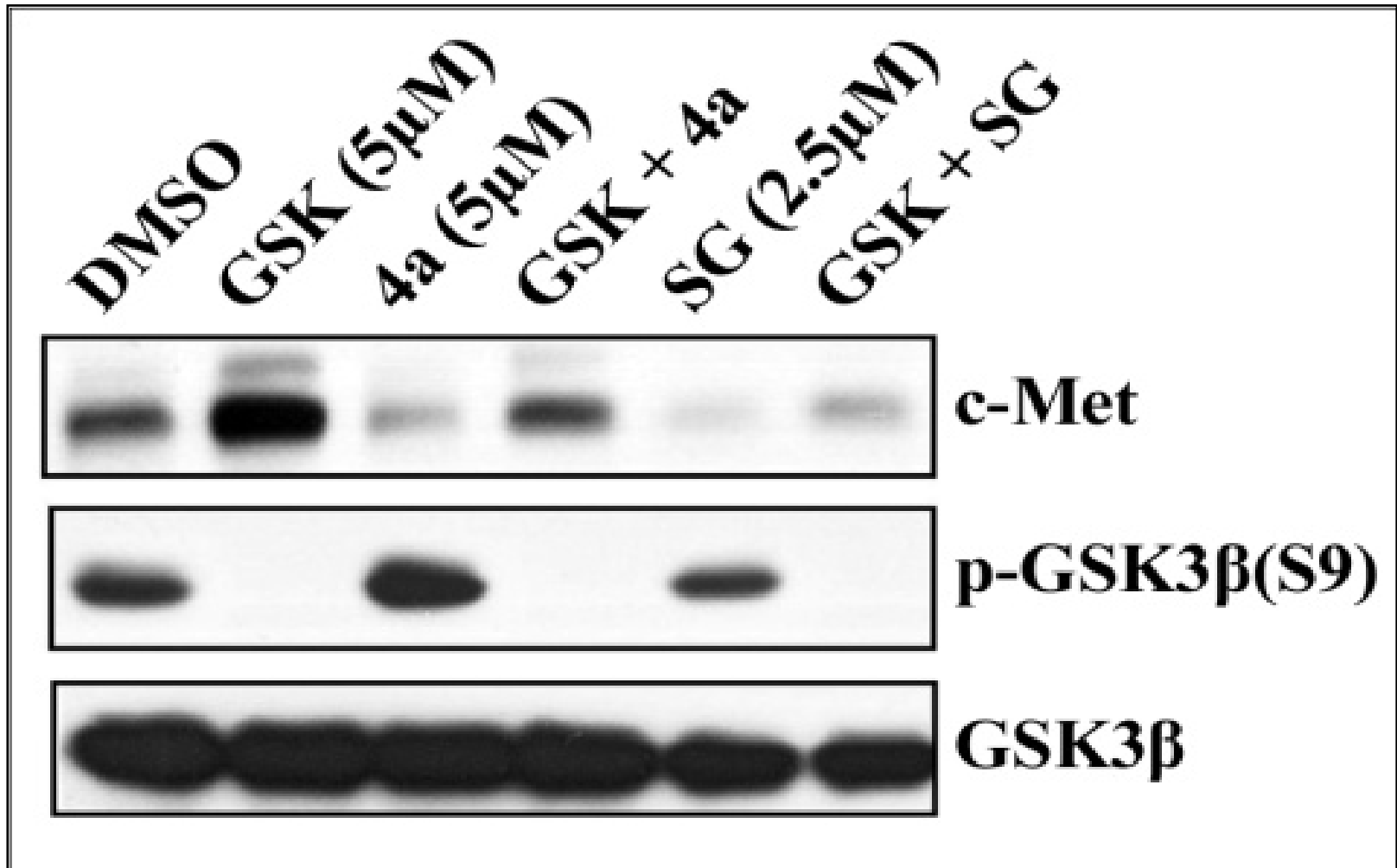


Figure 3b: Treatment of PC3-LN4 cells with Pim inhibitors decreases c-Met protein levels. Cells were treated with the indicated compounds for 24h and then extracts subjected to western blotting. GSK, GSK690693; 4a, SMI-4a; SG, Supergen 1776.

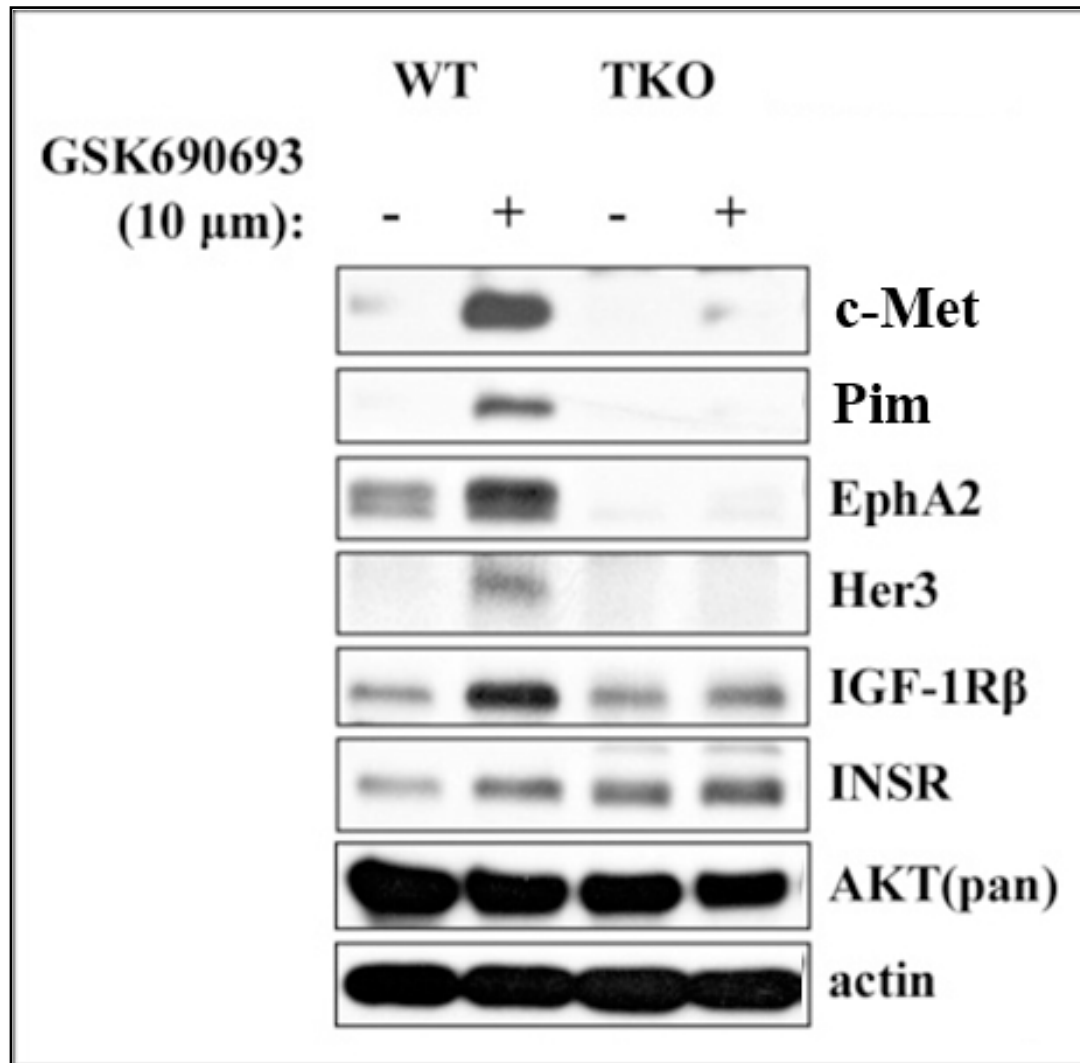


Figure 3c: AKTi do not induce RTKs in MEFs genetically engineered not to express any Pim isoform. WT MEFs and triple knock-out (TKO) MEFs were treated with GSK690693 for 24h and cellular extracts western blotted.

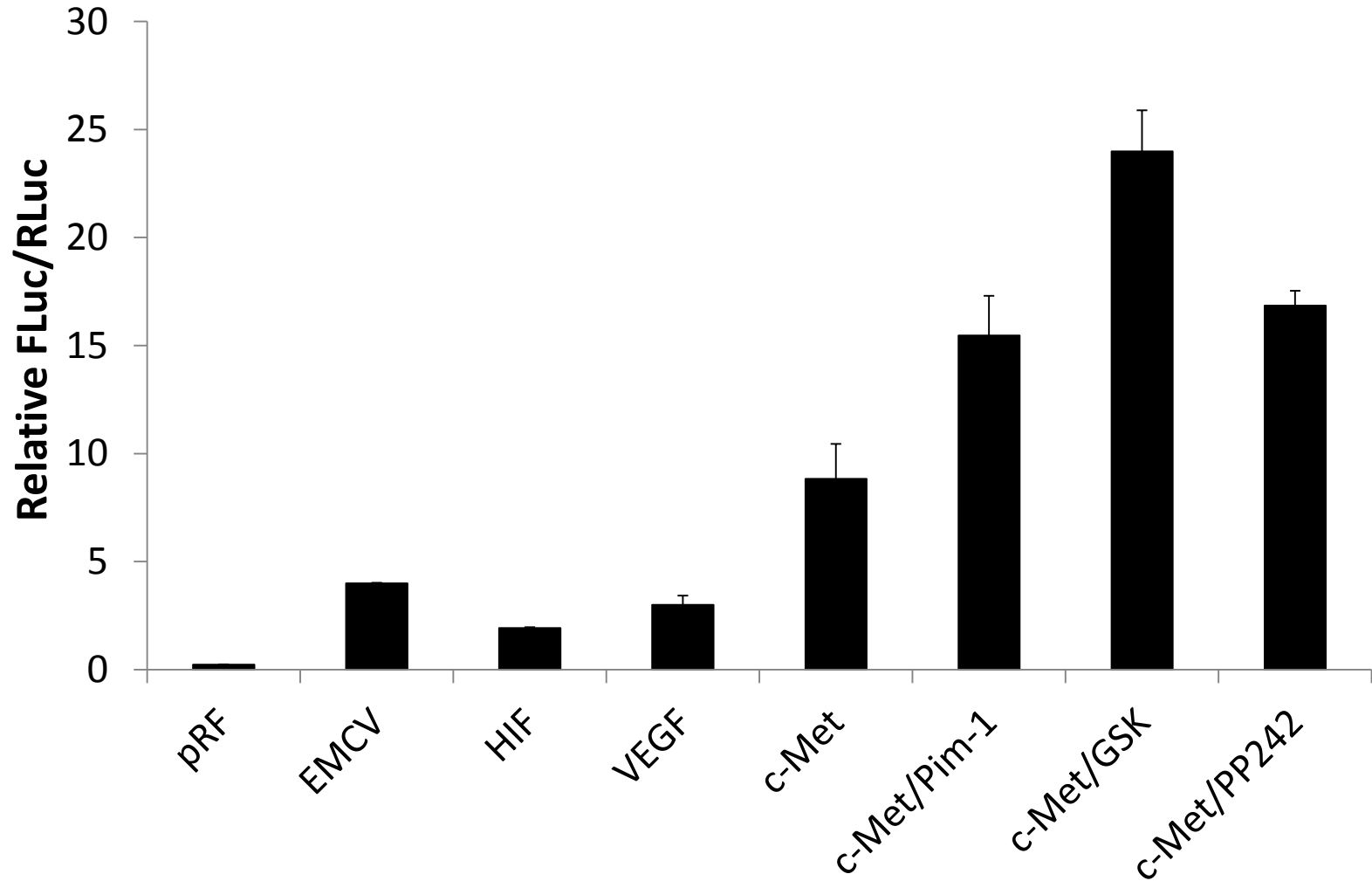


Figure 4: A vector containing an SV-40 promoter followed by renilla luciferase (RLuc) which was followed by the c-Met 5'UTR and a firefly luciferase (Fluc) reporter was transfected into PC3-LN4 cells with or without Pim-1 or GSK690693 treatment. The ratio of firefly to renilla luciferase is shown.

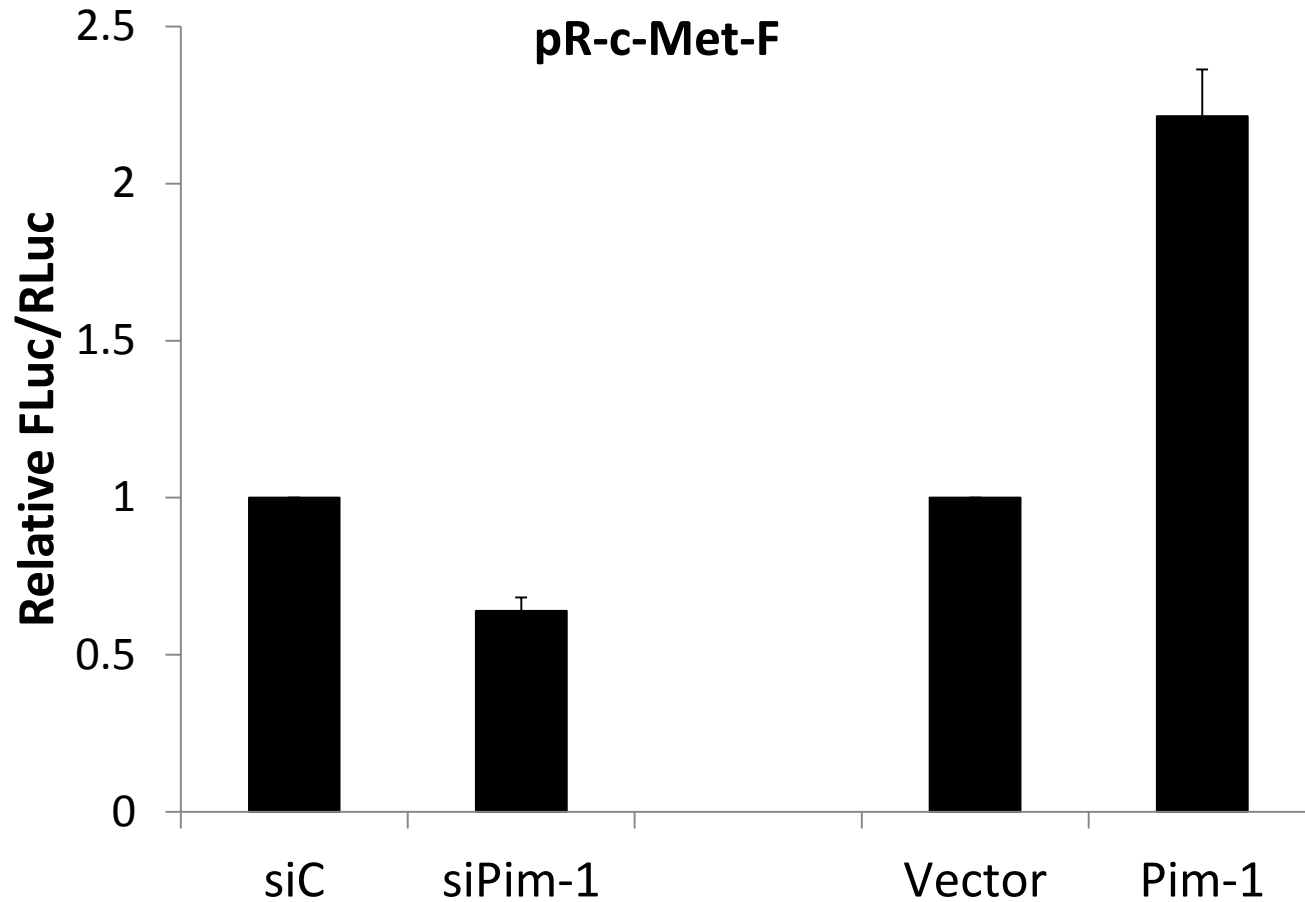


Figure 5: The plasmid as described was transfected into cells with Pim-1 or siRNAs directed at Pim-1. The assays were performed in triplicate and the average and standard deviations of these measurements are shown.

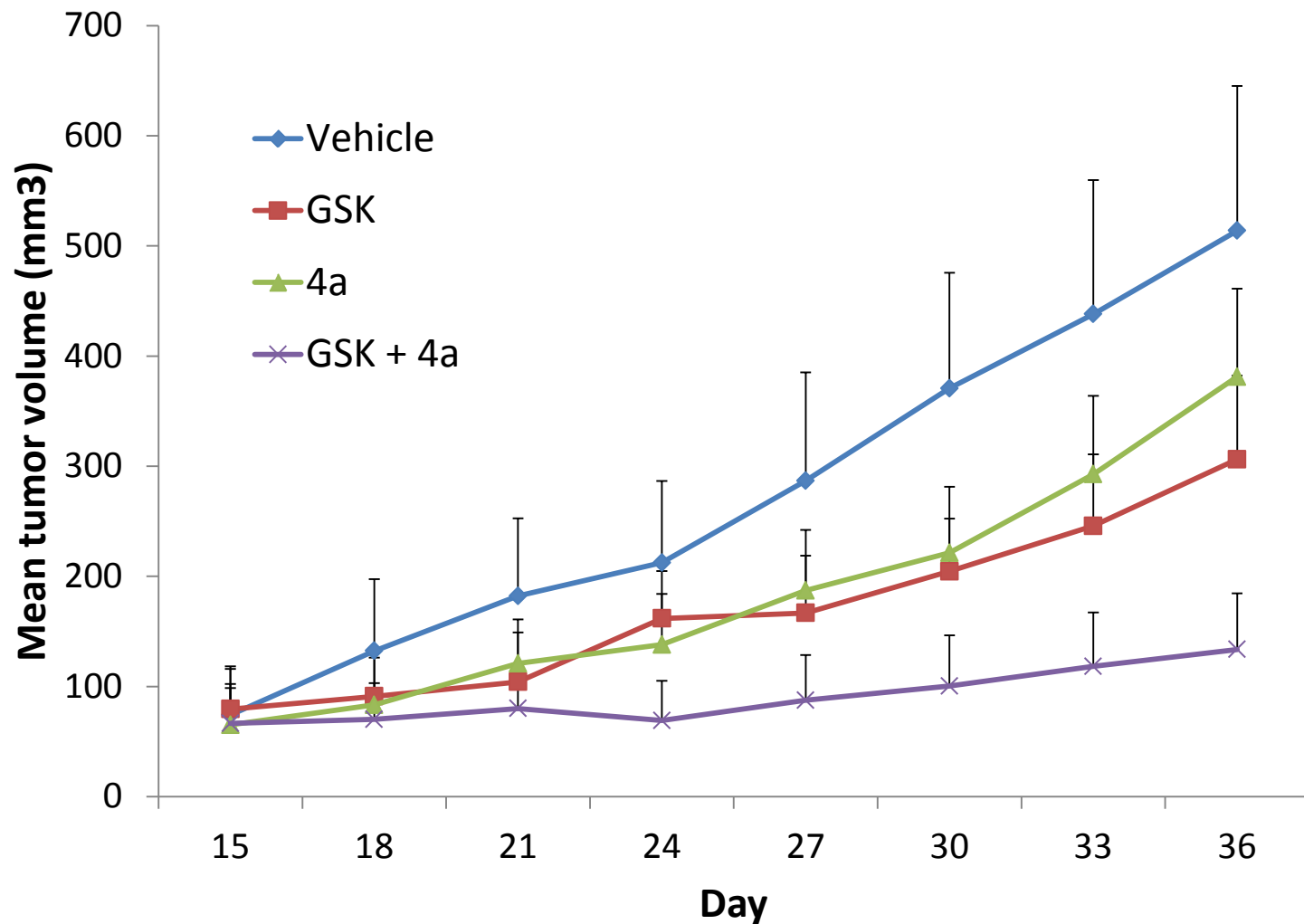


Figure 6: Combination therapy inhibits growth of PC3-LN4 tumors grown subcutaneously in immunocompromised mice. 40 NOD/SCID mice were injected with 1×10^6 PC3-LN4 cells. When tumors were visible on day 15 in groups of 10 they were treated with vehicle, either agent alone or the combination. The experiment was terminated on day 36. The mean size of the tumor \pm S.D. is shown.